UILU-ENG-71-2004

CIVIL ENGINEERING STUDIES

STRUCTURAL RESEARCH SERIES NO. 373

FATIGUE OF HIGH-YIELD-STRENGTH STEEL WELDMENTS

By J. B. Radziminski and F. V. Lawrence, Jr.

FATIGUE CRACK INITIATION AND PROPAGATION IN HIGH-YIELD-STRENGTH STEEL WELD METAL

By F. V. Lawrence, Jr. and J. B. Radziminski

Reprinted From

Welding Journal Research Supplement

UNIVERSITY OF ILLINOIS
AT URBANA-CHAMPAIGN
URBANA, ILLINOIS

Fatigue Crack Initiation and Propagation in High-Yield-Strength Steel Weld Metal

Flawed HY-130 butt welds are subjected to fatigue, and their total and crack propagation lives are measured and analyzed on the basis of a fracture mechanics analysis

BY F. V. LAWRENCE, JR. AND J. B. RADZIMINSKI

ABSTRACT. Full penetration, double-vee butt welds with reinforcement removed have been fabricated using a high-yield-strength steel, HY-130. Various filler metals and welding techniques were used. Most welds contained intentionally incorporated weld discontinuities such as slag, lack of fusion and/or porosity. Fatigue specimens were cut from these welds and tested in zero-to-tension, axial fatigue.

The point at which a fatigue crack began to propagate within the specimen was determined by radiographic measurements. The fatigue life of a specimen could therefore be separated into two parts—that portion spent in initiating a fatigue crack and that spent in fatigue crack propagation. The influence of flaw size and geometry upon the crack propagation portions of the fatigue life was found to be large and to depend upon the thickness of the member.

The results of these studies were found to be in good agreement with the fatigue lives predicted on the basis of a fracture mechanics analysis.

F. V. LAWRENCE, JR. is Assistant Professor, Depts. of Civil Engineering and Metallurgy and Mining Engineering, and J. B. RADZIMINSKI is Assistant Professor, Dept. of Civil Engineering, University of Illinois at Urbana-Champaign, Urbana, Ill.

Paper sponsored by ASME and presented at the AWS 51st Annual Meeting held in Cleveland, Ohio, during June 8-12, 1970.

Introduction

Since the introduction of the new high-yield-strength, heat-treated steels for welded structures, much attention has been given to the problem of designing welds which possess increased fatigue properties equal to those of the base metal. Recent investigations[1-3] have shown that the fatigue life of such welds may be substantially less than that of the base metal and hence restrict the usage of these high-strength materials in applications involving repeated loads, particularly repeated axial loads.

As shown in a companion paper,[4] a very large variation in fatigue life has been observed for welded high-strength steels fatigued at one stress level and failing at internal discontinuities. Attempts to relate this behavior to differences in base metal properties, filler metals, and variations in welding method have not been successful; it seems that these variables exerted little influence upon the fatigue phenomenon in these weldments. No strong correlation between any of these variables and the fatigue life expectancy of a weldment was found within the range of lives considered, i.e., approximately 10^4 to 10^6 cycles to failure.

The sizes of internal discontinuities present in the welds, on the contrary, had a large effect on the measured fatigue life: large defects usually resulted in a foreshortening of the expected fatigue lives, whereas minute defects often had a considerably less significant effect. The most important variable in determining the fatigue life of a flawed weldment would seem to be, therefore, the nature of the internal flaws contained within the weld and the manner in which these flaws interact with the stress field in the weld during its fatigue life.[5]

Fatigue Crack Propagation

The total fatigue life of a specimen can be divided into five phases: cyclic slip, crack nucleation, microcrack growth, macrocrack growth and failure.[6] For the purposes of the present study, the first three phases will be considered as the fraction of the fatigue life spent in crack initiation and

Table 1—Chemical Composition of HY-130 Base Metal (Data Supplied by U. S. Steel Corp.)

Heat number	5P2456	5P2004
Fatigue specimen designation	ND	NE
Chemical composition, %		
C	0.10	0.11
Mn	0.84	0.88
P	0.007	0.003
S	0.004	0.006
Si	0.24	0.35
Ni	4.92	4.95
Cr	0.54	0.53
Mo	0.50	0.50
V	0.08	0.08
Ti	0.04	—
Cu	0.06	0.07

Table 2—Mechanical Properties of HY-130 Base Metal (Data Supplied by U. S. Steel Corp.)

		Properties in Longitudinal Direction				
Heat number	Fatigue specimen designation	Yield strength,[a] ksi	Tensile strength, ksi	Elongation in 2 in., %	Reduction in area, %	Charpy V-notch, ft-lb 0° F
5P2456	ND	140.4	149.2	20.0	64.4	83
5P2004	NE	141.6	152.0	20.0	63.8	90

[a] 0.2% offset.

the latter two phases as the fraction of the fatigue life spent in crack propagation.

In terms of welds containing internal defects, the total fatigue life can be divided into an initiation period in which the defect does not enlarge perceptibly, and a propagation period in which a crack originating at the flaw enlarges until fracture has occured. In high-strength steel weldments tested at high stress levels, a significant portion of the fatigue life may be spent in fatigue crack propagation; consequently, there has been much recent interest in measuring the life spent in crack propagation and relating this life to that predicted using current theories of fracture mechanics.[7-11]

Purpose of the Present Investigation

The purpose of the present investigation was to measure the fatigue life of high-strength steel butt welds subjected to a uniform axial stress and containing various intentionally incorporated internal defects. This was done to determine the manner in which a particular defect influences the crack propagation in and the fatigue life of the weld. The point at which the defect became an active fatigue crack was detected by periodically interrupting testing and radiographing the specimen. In this manner the fraction of the fatigue life spent in crack propagation could be determined and compared with that predicted using fracture mechanics analyses.

Weld Fabrication and Testing Procedures

The specimens for this study were fabricated from a high-yield-strength quenched and tempered steel, HY-130. The chemistry and mechanical properties of the heats used are given in Tables 1 and 2. Two plate segments were cut from 1 in. thick plate stock and joined using a full penetration, multiple pass, double-vee butt weld. Both shielded-metal-arc and gas-metal-arc welding were used. The chemistries of the welding electrodes used are given in Table 3. In most specimens, the welding techniques were intentionally altered in such a way as to produce a specific defect area during a portion of one pass. This area was covered by successive passes in which no defects were intentionally created. Using the appropriate technique, internal defects such as slag, lack of fusion, and porosity of roughly the desired proportions could be created.

After welding, the plates were cut to the specimen shape shown in Fig. 1. In order to eliminate the possibility of toe initiated failures, the weld reinforcement was machined off of all specimens tested for this study. Furthermore, removing the reinforcement had the advantage of allowing more precise nondestructive inspection. After removing the reinforcement, the surfaces of all specimens were polished. Following their preparation, the specimens were examined using radiographic and ultrasonic inspection techniques to determine the type, concentration and position of the internal defects apparent within the weld prior to testing.

The specimens were inserted into a 200,000 lb capacity fatigue machine and cycled at a rate of approximately 150 cpm using stress cycles of 0 to 50 ksi, or 0 to 80 ksi axial tension. The tests were interrupted periodically to radiograph the weld to determine the onset of internal fatigue cracking or the extent of fatigue crack growth. Radiographs obtained at 10% intervals of the expected fatigue life permitted the determination of the point at which an internal fatigue crack began to propagate. Crack extensions of 0.02 to 0.05 in. could be detected by this procedure. From this information, the total fatigue life of a specimen could be separated into that spent in crack initiation (or early, undetected growth) and that spent in crack propagation.

All specimens were cycled until complete fatigue fracture occurred. Very little damage was imparted to the fracture surfaces, owing to the zero-to-tension stress cycle used; consequently it was possible to examine the fracture surfaces to determine the exact nature, size and position of the flaws initiating the fatigue crack.

Table 3—Chemical Composition of Electrodes for Welding HY-130 Plates

Manufacturer	U. S. Steel Corp.	Linde Div., Union Carbide Corp.	McKay Co.	
Electrode designation	5Ni-Cr-Mo	Linde 140	McKay 14018	
Electrode type	1/16 in. diam bare wire	1/16 in. diam bare wire	5/32 in. diam covered electrodes	3/16 in. diam
Heat number	50646	106140	1P1375	
Chemical composition, %			5/32 in. diameter	3/16 in. diameter
C	0.11	0.11	0.077	0.081
S	0.006	0.007	0.003	0.004
P	0.004	0.008	0.003	0.003
Mn	0.75	1.72	1.91	1.85
Si	0.38	0.36	0.42	0.39
Ni	5.03	2.49	2.08	1.92
Cr	0.61	0.72	0.71	0.73
Mo	0.47	0.88	0.43	0.43
V	0.01	0.01	—	—
Cu	—	0.08	—	—
Ti	0.015	—	—	—
Al	0.01	—	—	—
N	0.004	—	—	—

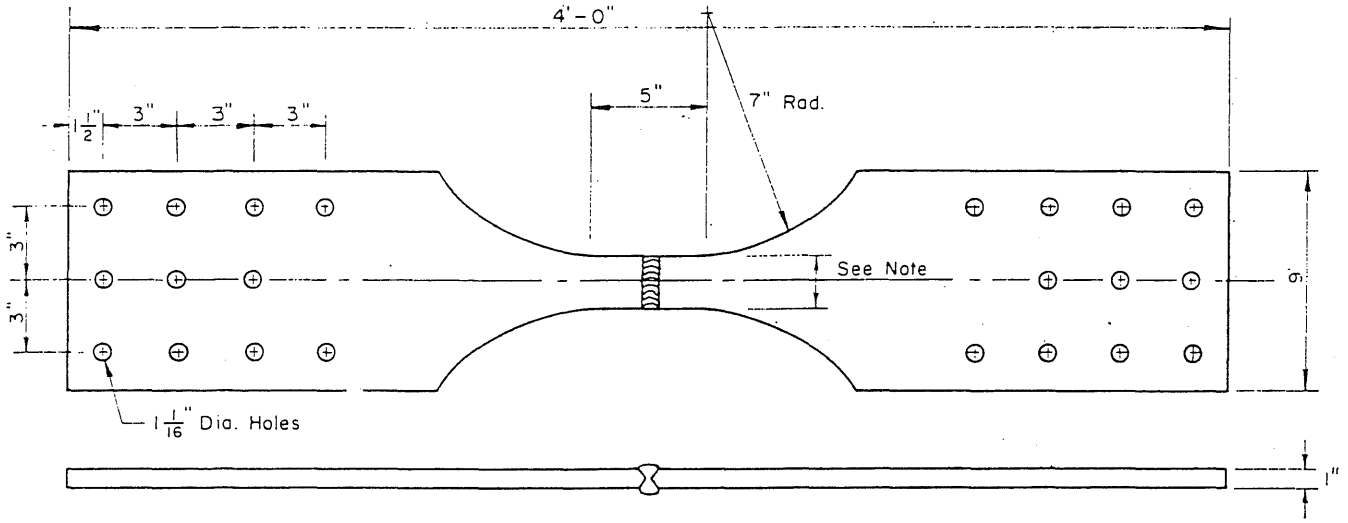

Fig. 1—Details of the butt welded fatigue test specimens. The weld reinforcement was removed prior to testing

Results of the Fatigue Crack Propagation Studies

The results of the fatigue tests of the welded HY-130 specimens are given in Table 4 and Fig. 2.

As can be seen in Fig. 2, there was considerable variation in the total fatigue lives measured at the two stress levels used, 0 to +50 ksi and 0 to +80 ksi. At 0 to +80 ksi, the total fatigue lives ranged from 1,500 cycles to 170,000 cycles or over two orders of magnitude. The spread in the lives at 0 to +50 ksi is almost as great; the lives ranged from 27,500 to 651,900 cycles or well over one order of magnitude in life.

The measured propagation lives, on the other hand, exhibit much less variation. At 0 to +80 ksi the propagation lives ranged from 2,250 to 9,300 cycles, less than one order of magnitude.* At 0 to +50 ksi, the propagation lives ranged from 14,500 cycles to 44,000 cycles, again, less than one order of magnitude.

The difference between the total lives and the measured propagation lives of a specimen is the number of cycles spent prior to crack initiation (or in undetected crack growth). For those specimens in which crack initia-

*The reason that some total lives are shorter than any propagation life shown in Fig. 2 is that the propagation life was not measured in all specimens reported; thus the propagation lives for some short total life specimens are missing.

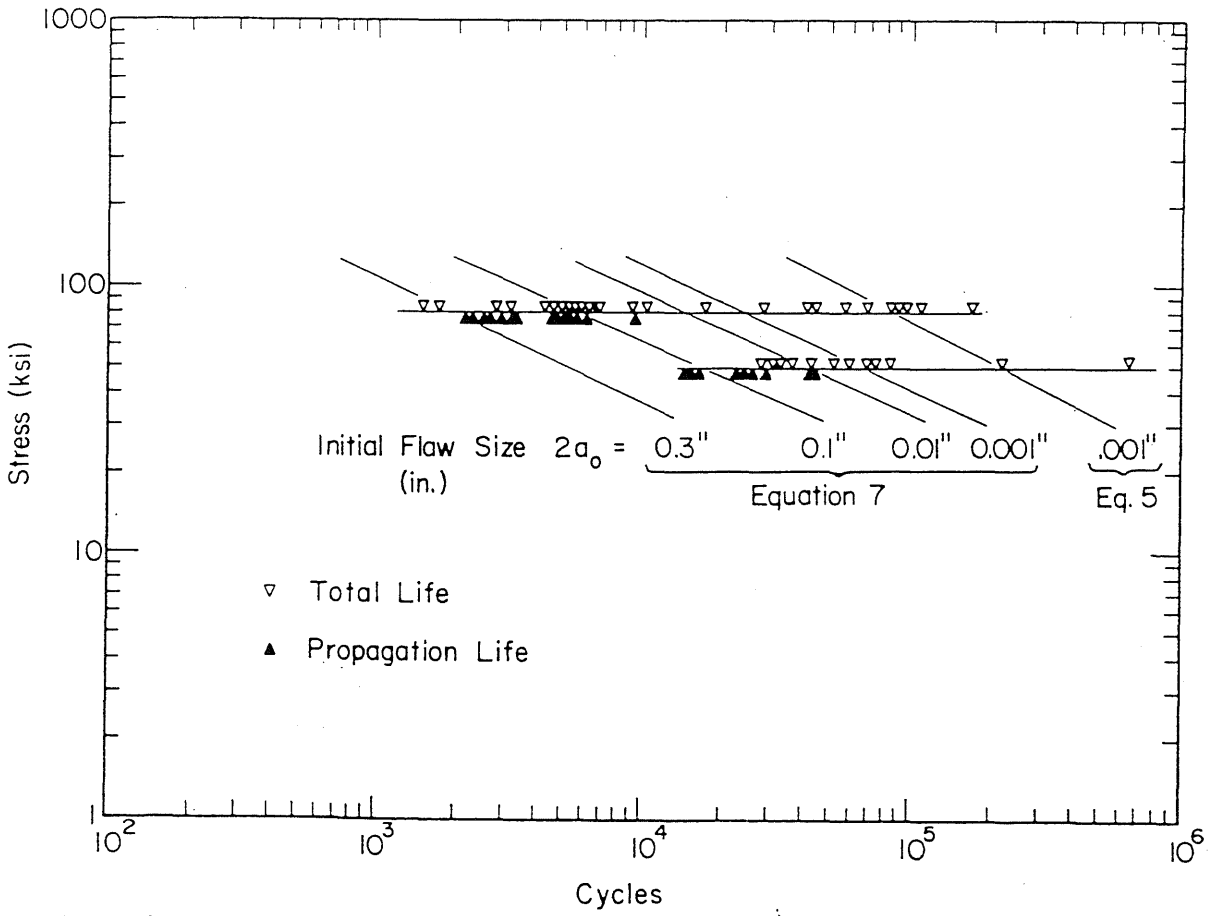

Fig. 2—Total and crack propagation portions of the fatigue life of HY-130 butt welds. The open triangles indicate the total lives while the solid indicate the propagation lives. The diagonal lines represent the predicted S-N curves (propagation) using the expression for a finite plate with a through crack (equation [7]) and the expression for a disc-shaped crack in an infinite body (equation [5])

tion and propagation was studied (see Table 4), the period of life spent in crack initiation varied from essentially zero cycles to over 38,000 cycles at 0 to +80 ksi and from essentially zero to over 74,000 cycles at 0 to +50 ksi.

As would be expected, the total lives and the number of cycles spent in crack initiation and propagation are smaller at the higher stress level than at the lower stress level. Also, there is a general, though not entirely consistent, correlation between large flaws and short fatigue lives as can be verified by inspection of Table 4 in which the dimensions of the flaws as measured on the fracture surface are given. It was found that the critical fatigue crack did not always start at the flaw which appeared to be most severe on the radiographs taken prior to testing. Often the fatal crack would start at a defect not evident upon the initial radiograph. These points are discussed more fully in a companion paper.[4]

Discussion

Fracture Mechanics Analysis

From the foregoing observations and the results of several recent studies,[7-10] it would seem reasonable that the effect of flaws on the fatigue life of welds could be related to the maximum stress experienced in the material adjacent to the defect, i.e., to the stress intensity associated with the defect. Moreover, it would seem that the type of the defect should have little effect upon the advancement of the fatigue crack, once initiated. The variation in the fraction of fatigue life spent in crack propagation shown in Fig. 2 is independent of the initial flaw type. Once an active fatigue crack has formed, the number of cycles to failure at any given stress level depends only upon the rate at which the crack propagates through filler metal and not upon the type of flaw initiating the crack, per se.

The rate at which a fatigue crack will advance has been studied extensively by Paris,[12] who showed that the rate of crack growth advance per cycle can be related to the range of stress intensity factor by the following equation:

$$\frac{da}{dn} = C(\Delta K)^n \qquad (1)$$

where:

$\frac{da}{dn}$ = rate of crack advance per cycle
C = material constant
n = material constant
ΔK = range of stress intensity factor.

Paris found that C and n remained constant over a wide range of stress intensity factors; other studies[13] have further shown that these constants vary little from one high-strength steel to another.

The range of stress intensity factor, ΔK, is a function of the crack width and stress level. Therefore, for tests conducted at a constant stress range, ΔK becomes a direct function of instantaneous crack length, and the number of cycles of propagation may be expressed as:

$$N = \int_{a_0}^{a_f} \frac{1}{C(\Delta K)^n}\, da \qquad (2)$$

where:

N = cycles spent in advancing the crack from a_0 to a_f
a_0 = half initial crack size (defect dimension in direction of subsequent crack growth)
a_f = half final crack size.

The number of cycles of repeated stress necessary to advance the crack from an initial flaw size $2a_0$ to a final crack size $2a_f$ can be calculated using equation (2) if an analytical function for the range of stress intensity factor can be found and integrated. In those cases where the integration of equation (2) is difficult, a finite difference technique can be used and the integration performed numerically with the aid of a computer.

$$N = \sum_{a_0}^{a} \frac{\Delta a}{C(\Delta K)^n} \qquad (3)$$

where:

Δa = small finite advance of the crack.

Using either equation (2) or (3) and letting a_f equal half the thickness of the specimen, it is possible to estimate the number of cycles spent in crack propagation during the fatigue life of a weld if the initial flaw size in the through-thickness specimen direc-

Table 4—Results of Crack Propagation Studies[a]

Specimen number	Stress cycle, ksi	Crack propagation life, cycles	Total life, cycles	Defect type	Defect length, in.	Defect width, in.	Defect position, in. from surface	Welding procedure and filler metal
ND-8	0–50	14,500	59,500	L	.97	.05	.50	U
ND-21	0–50	16,300	43,800	V	.35	0.2	.40	U
ND-20	0–50	31,000	36,000	LP	.30	.06	.38	U
ND-12	0–50	44,200	219,200	LP	.52	.04	.50	L
ND-28	0–50	+	72,300	L	.50	.125	.28	L
ND-10	0–50	22,500	27,500	L	.65	.05	.37	L
ND-18	0–50	23.800	83,800	S	.55	.05	.46	M
ND-17	0–50	43,800	71,300	S	.95	.10	.36	M
ND-19	0–50	34.500	52.000	S	.70	.07	.36	M
ND-14	0–50	15,000	33,500	P	.175	.175	.27	M
ND-15	0–50	25,400	32,400	P	.08	.08	.26	M
ND-25	0–50	+	651,900	P	.05	.05	.50	M
ND-9	0–80	+	170,000	P	<.001	<.001	.44	U
ND-6	0–80	9,300	95,300	P	<.001	<.001	.50	U
ND-26	0–80	+	95,000	L	.10	.05	.20	U
ND-22	0–80	+	69,000	P	<.001	<.001	.38	U
ND-24	0–80	+	17,800	V	.35	.025	.32	U
ND-13	0–80	+	110,000	P	.03	.03	.35	L
ND-11	0–80	+	4,300	L	1.05	.12	.28	L
ND-16	0–80	+	6,200	S	.30	.02	.40	M
ND-27	0–80	+	86,300	P	<.001	<.001	.50	L
ND-43	0–80	+	28,900	P	.04	.04	.50	L
ND-41	0–80	2,530	9,030	L	.94	.175	.33	L
ND-36	0–80	6,100	6,600	L	.35	.16	.30	L
ND-44	0–80	4,550	5,800	L	.40	.08	.29	L
ND-37	0–80	4,600	5,600	L	.45	.10	.36	L
ND-40	0–80	2,380	5,380	V	.6	.10	.50	L
ND-42	0–80	+	4,450	L	.58	.10	.35	L
NE-10	0–80	2,250	3,250	L	.96	.05	.35	L
NE-9	0–80	+	1,760	L	.74	.08	.29	L
ND-39	0–80	+	1,500	L	1.17	.20	.41	L
ND-46	0–80	4,850	42,850	S	.18	.05	.25	M
ND-47	0–80	4,950	10,400	S	.06	.05	.32	M
ND-45	0–80	5,730	6,750	S	.22	.08	.35	M
ND-38	0–80	5,200	5,700	S	.06	.04	.24	M
NE-8	0–80	3,220	4,970	S	.44	.02	.50	M
NE-7	0–80	2,620	2,870	S	.12	.09	.40	M
NE-11	0–80	3,230	4,830	P	.01	.01	.22	M
NE-12	0–80	2,900	4,400	S	.50	.08	.41	M

[a] Symbols: +—not measured; S—slag; P—porosity; V—void; L—lack of fusion; LP—lack of penetration; U—United States Steel; L—Linde; M—McKay.

tion, $2a_o$, is known, the material constants C and n are known, and if an analytical function for the range of stress-intensity factor can be found which fits the geometry and/or boundary conditions of the physical situation.

Although exact solutions for a generalized flaw in a finite body are not available, solutions for simpler cases which bound or closely model most physical situations do exist.

A very simple model for a flaw in a weld, a disc-shaped crack in an infinite body, is shown in Fig. 3a. The range of stress intensity for a zero-to-tension stress condition (stress perpendicular to the plane of the crack) would be:[12]

$$\Delta K = \frac{2}{\pi}\sigma\sqrt{\pi a} \qquad (4)$$

where:

σ = maximum tensile stress

a = crack radius or half width.

Substituting this function into equation (2) and integrating:

$$N = \frac{a_f^{(1-n/2)} - a_0^{(1-n/2)}}{\left(1-\frac{n}{2}\right) C \left(\frac{2\sigma}{\sqrt{\pi}}\right)^n}. \qquad (5)$$

A second model, that of a through crack in a body which is finite in the direction of crack advance is shown in Fig. 3b. The range of stress intensity for a zero-to-tension stress situation can be expressed as:[14]

$$\Delta K = \sigma\sqrt{\pi a}\left(\sec\frac{\pi a}{2b}\right)^{1/2}, \quad 0 \le a \le 0.8b \qquad (6)$$

where b = plate half thickness.

Substituting this function (equation (6)) into equation (3):

$$N = \sum_{a_0}^{a_f}\left[\frac{\cos\frac{\pi a}{2b}}{a\,C^{2/n}\,\sigma^2\,\pi}\right]^{n/2}\Delta a. \qquad (7)$$

In Fig. 4 models of various types of flaws commonly encountered in welds are shown. The through crack of Fig. 3b, for which equations (6) and (7) were developed, models the continuous and intermittent linear flaws shown in Figs. 4a and 4b quite closely; but, it does not adequately model the small, isolated pore. The disc-shaped flaw of Fig. 3a, for which equations (4) and (5) were developed, is more realistic for the latter case. One characteristic of both equations (5) and (7) is that the crack propagation life calculated is very sensitive to the choice of initial flaw size, a_o. A fatigue crack spends the major portion of its propagation life as a very small crack and the accuracy of the solution will therefore depend in large part upon accurately modeling the initial size and geometry of the defect (see Fig. 5).

Comparison with Experimental Results

As reasoned above, the initial size (in the direction of subsequent propagation) and, to a lesser extent, the geometry of a flaw should determine the length of the crack propagation period of the fatigue life. The fatigue lives of Table 4 and Fig. 2 have

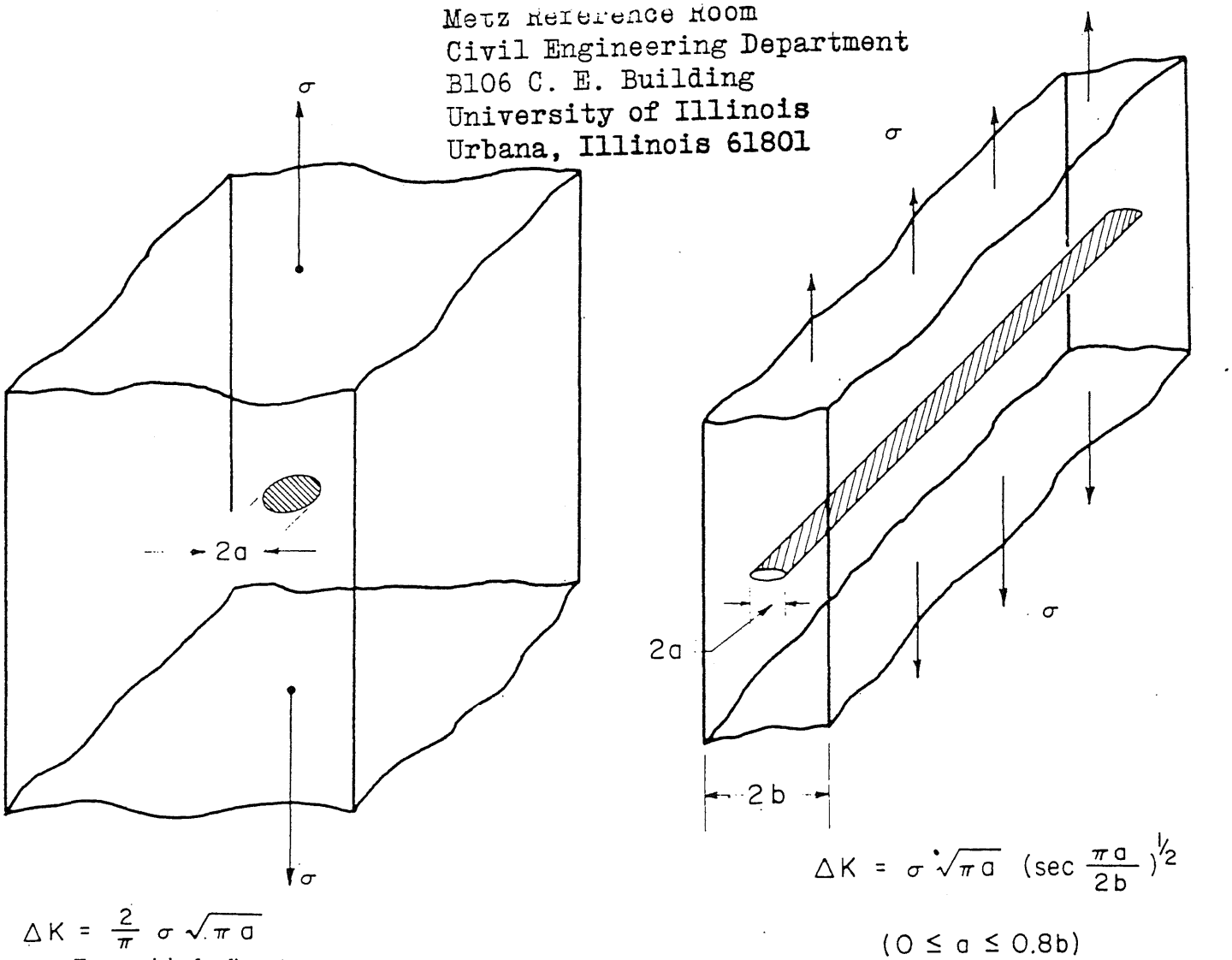

Fig. 3—Two models for flawed weldments: left (a)—a disc-shaped crack in an infinite body; right (b)—a through crack in a finite plate. The stress intensity factors are given for each

therefore been replotted as a function of initial flaw size for the two stress levels of 0 to +80 ksi and 0 to +50 ksi in Figs. 6 and 7. The initial flaw size $2a_o$ in these plots is the initial width of the largest flaw seen on the fracture surface of each specimen. This dimension has been plotted against the total fatigue life, and, for those specimens in which propagation measurements were taken, against the life spent in crack propagation as determined experimentally by radiography. The propagation and total lives measured for a specimen have been connected by a horizontal line, the length of which is the life apparently spent in initiating an active fatigue crack (or in undetected, early crack growth).

Also appearing in Figs. 6 and 7 are three curves for the life spent in crack propagation, N, which have been calculated using equations (5) and (7). The values of C and n used in these calculations are those determined by Barsom, Imhof and Rolfe[13] for HY-130 steel using a zero-to-tension stress cycle and 1 in. thick wedge-opening-loading (WOL) specimens, conditions which are, with the exception of specimen geometry, similar to those used in the present study.

At 0 to +80 ksi the total lives and, particularly, the propagation lives, lie within a band that straddles the predicted results calculated using the through crack in a finite plate model, equation (7). This model represents a condition of severity at least equal to that of the most critical flaw encountered in this study (continuous lack of fusion, etc., see Fig. 4). The fact that some of the specimens exhibited propagation lives less than those predicted by equation (7) may be explained in part by the limitations of the nondestructive testing techniques used to detect crack initiation; i.e., crack extensions of less than about 0.03 in. were generally undetectable on a radiograph, which could result in appreciable error in the estimation of life spent in propagation. It is more difficult to explain why the *total* lives of some of the test specimens were less than the propagation lives predicted by equation (7).

A possible explanation for the shorter lives may be that most flaws were not positioned along the center-line of the weld as assumed for equation (7), but were actually asymmetrically located. The position of the center of the flaw relative to the surface of the specimen is given in Table 4. The centers of some flaws are more nearly at the quarter-points of the specimen. With such flaws, the stress intensity factor for the edge nearest the surface of the specimen is greater than that assumed in the calculation of equation (7) for a 1 in. thick plate. Consequently, a fatigue life shorter than that predicted above could result. The magnitude of this effect can be assessed by bounding the problem with the solution of equation (7) for a $^1/_2$ in. thick plate, the assumption being that a flaw of $2a_o$ initial width with its center at 0.25 in. from the surface of a 1 in. plate could be similar to but not worse than a flaw of $2a_o$ initial width at the center-line of a $^1/_2$ in. plate.

Curves for this latter condition are also plotted in Figs. 6 and 7; it can be seen that the differences between the solution for a 1 in. thick and $^1/_2$ in. thick plate are most pronounced at the larger flaw sizes. For very small flaw sizes the solutions are essentially identical because the effect of the boundary conditions upon the flaw's initial behavior is small. The solution for the $^1/_2$ in. plate very nearly bounds all the data.

The smallest defects which have been observed to initiate fatigue cracks were very small pores. The initial geometry of and the boundary conditions for these flaws may be conservatively approximated by the disc-shaped crack in an infinite body model assumed in equation (5). The difference between the curves for equations (7) and (5) (in Fig. 6) at small flaw sizes reflects the effect of the difference in geometry between point and line flaws. Consequently, the curve for equation (5) should rep-

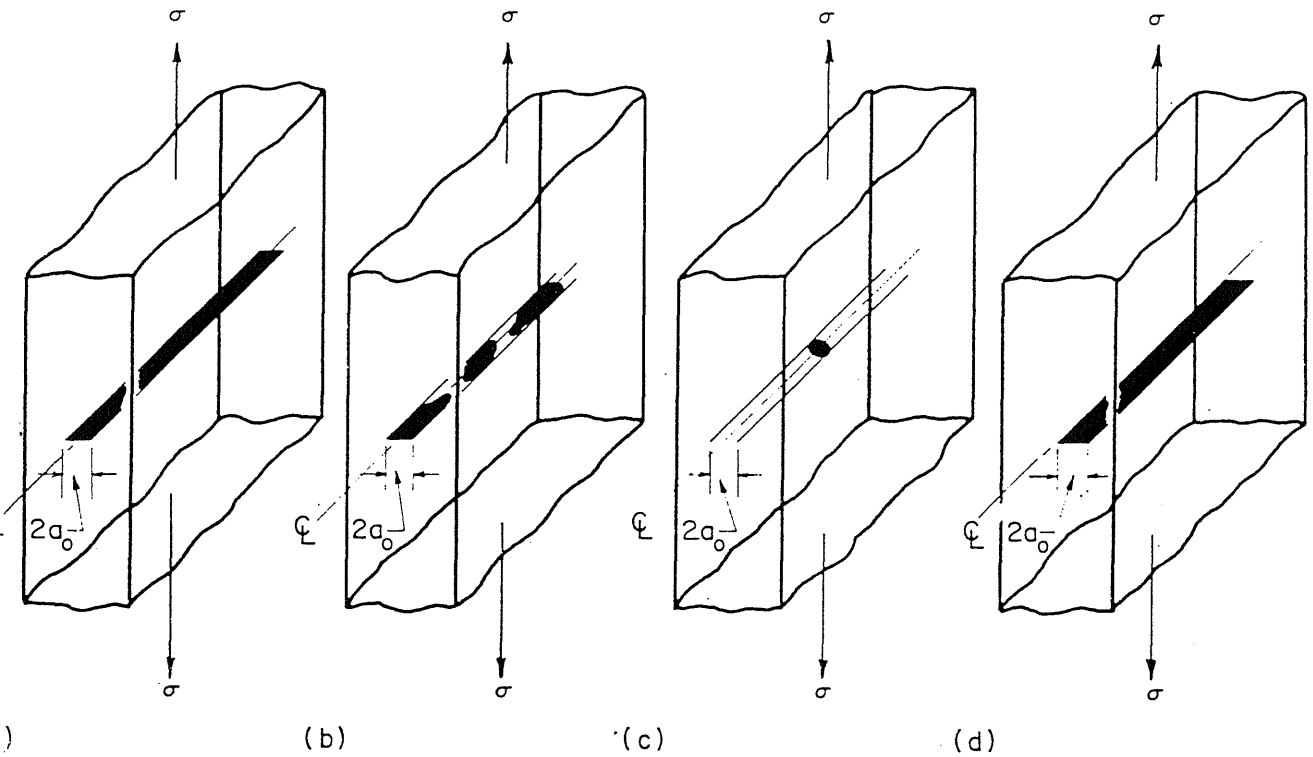

Fig. 4—Types of flaws found in weldments: (a) continuous linear defects at the center of the weldment, e.g., lack of fusion, continuous slag; (b) intermittent linear defects at the center of the weldment, e.g., intermittent lack of fusion, intermittent slag, elongated porosity; (c) isolated pores at the center of the weldment, e.g., small voids, pores, very small defects of all kinds; (d) continuous linear defects located off center in the weldment

resent the propagation life of very small isolated pores better than should equation (7). As can be seen in Fig. 6 the plot of equation (5) bounds most of the fatigue data and agrees particularly well with the fatigue lives of the smallest (spheroidal) defects initiating fatigue fracture.

The same general remarks apply to the data presented in Fig. 7 for tests conducted at 0 to +50 ksi. Few lives were recorded less than that predicted by equation (7) for a 1 in. thick plate. The data for the most part lie between the curves for equations (7) and (5).

The two models used in the fracture mechanics analysis can be seen to bound the data measured at both stress levels, as shown in Fig. 2. S-N curves based on various initial flaw widths have been plotted using the results of equations (5) and (7). Most of the measured fatigue data lie between the solution of equation (7) for an initial flaw size $2a_0$ of 0.3 in. and equation (5) for an initial flaw size $2a_0$ of .001 in.

Conclusion

The results of this study show the large effect internal weld defects may have upon the fatigue life of high-yield-strength steel welds cycled under axial loads. Their fatigue lives have been shown to be insensitive to the welding technique and filler metal used, but highly sensitive to the size and geometry of the flaw initiating fracture.

Measurements of the point at which an observable fatigue crack began to propagate within the specimen have confirmed that a large fraction of the fatigue life is spent in crack propagation—and, particularly at higher stress levels and for larger defect sizes, the crack propagation period may in fact constitute almost the entire fatigue life of the specimen.

The results of the experimental por-

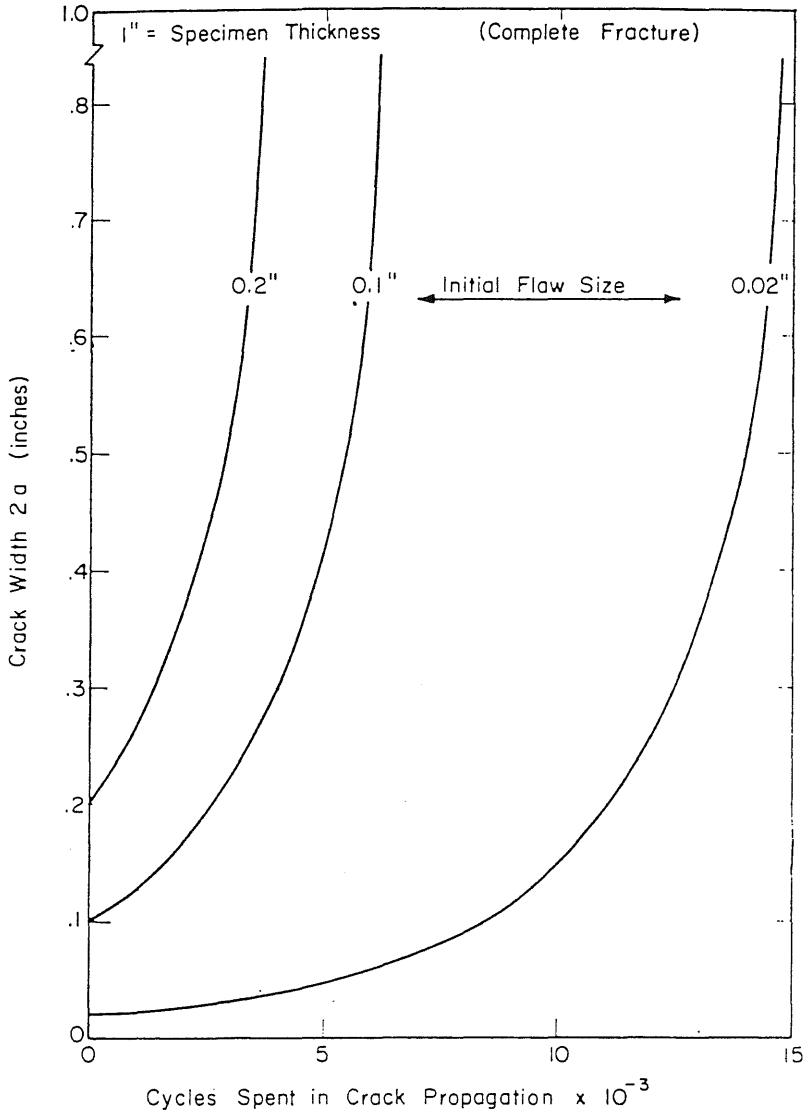

Fig. 5—Effect of initial flaw size on the crack propagation life of a flawed 1 in. thick HY-130 weldment

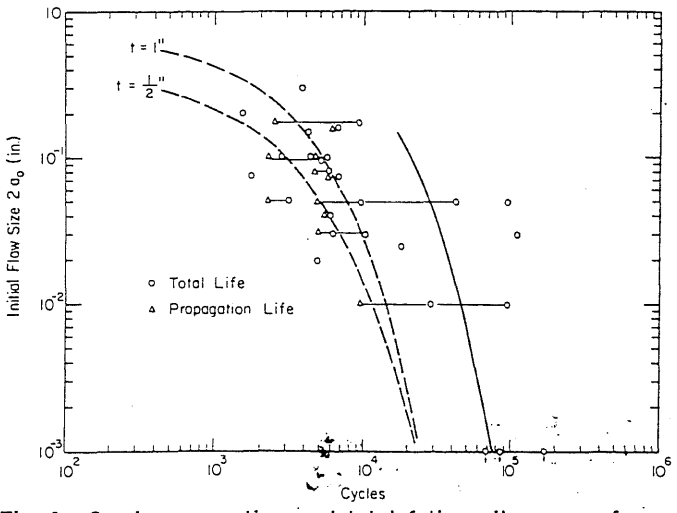

Fig. 6—Crack propagation and total fatigue lives as a function of initial flaw size (width) $2a_0$ at 80 ksi stress level. The dashed lines are solutions of equation (7) (finite plate-through crack) for 1 and ½ in. plate thicknesses. The solid line is a solution for equation (5) (infinite body-disc shaped crack). The horizontal lines connect the propagation and total lives of one specimen

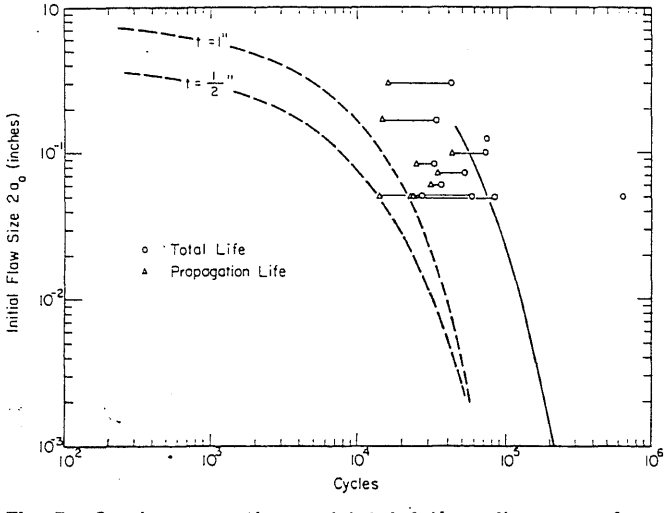

Fig. 7—Crack propagation and total fatigue lives as a function of initial flaw size (width) $2a_0$ at 50 ksi stress level. The dashed lines are solutions of equation (7) (finite plate-through crack) for 1 and ½ in. plate thicknesses. The solid line is a solution of equation (5) (infinite body-disc shaped crack). The horizontal lines connect the propagation and total lives of one specimen

tions of this study have been compared with the propagation lives calculated using the concepts and equations of fracture mechanics. The data agree well with these theories and several conclusions may be drawn from the theoretical and experimental results:

1. The effect of flaw width and the ratio of flaw width to plate thickness are dominant in controlling the length of the period spent in crack propagation.

2. The position of the flaw relative to the center-line of the weld is an important parameter in determining the propagation life. Larger flaws positioned off the center-line of the weld should propagate to failure more rapidly than ones located in exactly the middle of the plate. For very small flaws this is not as important an effect.

3. At very small flaws, where the fineness of the plate does not affect the flaw during its early stages of crack propagation, the actual geometry of the flaw, i.e., whether it is elongated or spherical, is influential in determining the propagation life. For flaws which are large relative to the plate thickness, the geometry of the flaws influences the propagation life only to a minor extent.

Further study and more refined experimental techniques will be required to determine accurately the period of life spent in initiating an active fatigue crack and the role of flaw size, flaw geometry and stress level in determining that life.

Until such time as the factors controlling this initiation period are better understood and permit the length of that period to be predicted, the fatigue lives of high-strength steel weldments failing at internal flaws may be estimated by neglecting the crack initiation period and using the concepts of fracture mechanics to (empirically) predict the number of cycles spent in crack propagation and hence the minimum expected total life. Furthermore, from the demonstrated sensitivity of the propagation life to initial width of the flaw, it would seem that the fatigue life of a weldment in service should be assumed to be no better than that resulting from the largest flaw (through-thickness dimension) which may be permitted or remain undetected by the post fabrication nondestructive inspection standards used.

Acknowledgments

The tests reported in this study are the result of an investigation conducted in the Civil Engineering Department of the University of Illinois at Urbana-Champaign, Urbana, Illinois. The program was supported by funds provided by the Naval Ship Systems Command, U.S. Navy.

This investigation constitutes a part of the structural research program of the Department of Civil Engineering, of which Dr. N. M. Newmark is the Head. The program was conducted under the general supervision of W. H. Munse, Professor of Civil Engineering.

The authors wish to thank the many staff members at the University who have assisted in the conduct of this investigation.

References

1. Radzimski, J. B., Lawrence, F. V., Jr., Mukai, S., Panjwani, P. N., Johnson, R., Mah, R., and Munse, W. H., "Low Cycle Fatigue of HY-130(T) Butt Welds," Civil Engineering Studies, Structural Research Series No. 342, University of Illinois, Urbana, Illinois, December 1968.

2. Radziminski, J. B., Lawrence, F. V., Jr., Wells, T. W., Mah, R. and Munse, W. H. "Low Cycle Fatigue of Butt Weldments of HY-100(T) and HY-130(T) Steel": Civil Engineering Studies, Structural Research Series No. 361, University of Illinois, Urbana, Illinois, July 1970.

3. Boblenz, T. L., and Rolfe, S. T., "Low Cycle Fatigue Characteristics of HY-130(T) Weldments," Applied Research Laboratory Report No. 39.018-006(6), United States Steel Corporation, Monroeville, Pa., June 1, 1967.

4. Radziminski, J. B., and Lawrence, F. V., Jr., "Fatigue of High-Yield-Strength Steel Weldments," WELDING JOURNAL, 49(8), Research Suppl., 365-s to 375-s (1970).

5. Ottsen, H., "Three-Dimensional Photoelastic Investigation of Simulated Weld Discontinuities," Doctoral Thesis, Department of Civil Engineering, University of Illinois, Urbana, Illinois, 1970.

6. Schijve, J., "Significance of Fatigue Cracks in Micro-Range and Macro-Range," *Fatigue Crack Propagation,* American Soc. Testing Materials, STP No. 415, 1967.

7. Burdekin, F. M., Harrison, J. D., and Young, J. G., "The Effects of Weld Defects with Special Reference to BWRA Research," *Welding Research Abroad,* Volume XIV, No. 7, August-September 1968 (reprint from the *Australian Welding Journal,* January 1968).

8. Harrison, J. D., "The Analysis of Fatigue Results for Butt Welds with Lack of Penetration Using a Fracture Mechanics Approach," *Fracture* 1969, Proceedings of the Second International Conference on Fracture, Brighton, April 1969.

9. Fisher, J. W., Frank, K. H., Hert, M. A., and McNamer, B. M., "Effect of Weldments on the Fatigue Strength of Steel Beams," Fritz Engineering Laboratory, Department of Civil Engineering, Lehigh University, September 1969.

10. Sinclair, G. M., and Rolfe, S. T., "Analytical Procedure for Relating Subcritical Crack Growth to Inspection Requirements," Applied Research Laboratory, Report No. 39.018-007(26), United States Steel Corporation, Monroeville, Pa., January 1969.

11. Miller, G. A., "The Dependence of Fatigue Crack Growth Rate on the Stress Intensity Factor and the Mechanical Properties of Some High-Strength Steels," Trans. ASM, Vol. 61, 1968.

12. Paris, P. C. and Sih, G. C., "Stress Analysis of Cracks," *Fracture Toughness Testing and Its Applications,* ASTM STP No. 381, 1965.

13. Barsom, J. M., Imhof, E. J., and Rolfe, S. T., "Fatigue-Crack Propagation in High-Strength Steels," Applied Research Laboratory, Report No. 39.018-007(27), United States Steel Corporation, Monroeville, Pa., December 1968.

14. Feddersen, C. E., Discussion to "Plane Strain Crack Toughness Testing of High Strength Metallic Materials," by Brown, W. F., and Srawley, J. E., ASTM STP No. 410, 1967.

Fatigue of High-Yield-Strength Steel Weldments

Cyclic response studies for three high-yield-strength steels reveal marked differences in behavior between butt welds exhibiting toe failures and those initiating cracking at internal weld discontinuities

BY J. B. RADZIMINSKI AND F. V. LAWRENCE, Jr.

ABSTRACT. An investigation of the fatigue resistance, under uniaxial loading, of plain plates (mill-scale intact) of three high-yield-strength steels—HY-80, HY-100 and HY-130—has indicated that the cyclic behavior of all three materials may be reasonably described by the same S-N curve within the range of lives from approximately 10^4 to 10^6 cycles. A similar uniformity of response was observed for full penetration butt welds fabricated using each of the base metals, and in which fatigue failures initiated at the toe of the weld reinforcement.

In contrast, considerable scatter in fatigue lives was encountered at a particular stress level for weldments in which fatigue crack initiation occurred at internal weld discontinuities. This scatter could not be attributed solely to the type of defect present at the crack initiation site as described either by NDT inspection prior to testing or from examination of the fracture surface after failure. Further, it was found that one- or two-dimensional radiographic descriptions of weld defect size and arrangement, commonly used as a measure of defect severity with respect to structural integrity under a single load application, could not be used to reliably estimate the total fatigue response of weldments containing one or more detected defects.

Introduction

Object and Scope of Investigation

There has been considerable interest in recent years in the development of steels of increasingly higher strengths intended for a variety of welded structural applications. Of prime concern in the evaluation of candidate steels has been the requirement that the weldments exhibit satisfactory performance under various environments and service loading histories. The present study was undertaken to evaluate the behavior, under repeated loads, of both plain plates and butt-weldments prepared using three grades of heat-treated steel with minimum nominal yield strengths of 80,000, 100,000 and 130,000 psi.

To examine the relative influence of differences of material and geometry on the fatigue resistance of weldments of the three steels, specimens were fabricated from plates varying in thickness from $^1/_2$ to $1^1/_2$ in. using, where possible, welding procedures representative of field practice. The specimen types investigated included plain plates with the mill-scale intact (referred to herein as "as-rolled"), surface-treated plates, and full penetration butt weldments tested both as-welded and with the weld reinforcement removed. Additionally, several series of the butt welds were prepared with intentionally induced defects, slag, porosity, incomplete fusion, etc., to determine the relative influence of these defects on the fatigue resistance of the welded details.

The fatigue tests were conducted using constant stress amplitude, uniaxial loadings with the imposed stress levels adjusted to produce fatigue lives in the range from several thousand to several hundred thousand cycles. The lives obtained for weldments exhibiting internal crack initiation have been compared with S-N curves determined for base metal specimens and for weldments in which failure initiated at the toe of the weld. An attempt has been made also to relate internal defect type and size with fatigue behavior.

Material

Three grades of high-yield-strength steel were used in the study: HY-80, HY-100 and HY-130. The chemical composition and mechanical properties of the various heats of each of the steels are presented in Tables 1 and 2, respectively.

For the weldments fabricated using the HY-80 and HY-100 steels, manual shielded metal-arc welding was utilized, while both shielded metal-arc and gas metal-arc welding processes were used in the preparation of the HY-130 weldments. The majority of the HY-80 specimens were fabricated with E11018 covered electrodes; both E12018 and E11018 electrodes were used for the HY-100 weldments. Three bare wire electrodes and one covered electrode were used in the preparation of the HY-130 welded specimens. The chemical composition of each of the HY-130 filler metals is given in Table 3.

Specimen Preparation

Full penetration, double-vee groove welds were used for the welded fatigue specimens. Typical welding conditions for the fabrication of specimens using both the shielded metal-arc and gas metal-arc processes are listed in Table 4. For weldments using each of the procedures of Table 4, static tensile test specimens prepared in accordance with NAVSHIPS 0900-006-9010[1] exhibited failure in the base metal, demonstrating an acceptable overmatching of the strength of the weld metal to that of the base metal. All of the procedures produced welds of sufficient ductility to withstand a 180 deg bend without cracking when subjected to sidebend tests using a mandrel radius of 2t.

The same welding procedures as those presented in Table 4 were used to prepare the test weldments containing intentional defects, except that

J. B. RADZIMINSKI is Assistant Professor, Dept. of Civil Engineering, and F. V. LAWRENCE, Jr., is Assistant Professor, Depts. of Civil Engineering and Mining and Metallurgical Engineering, University of Illinois, Urbana-Champaign, Ill.

Paper sponsored by the Metals Engineering Division of ASME and presented at the AWS 51st Annual Meeting held in Cleveland, Ohio, during June 8-12, 1970.

Opinions and assertions contained in this paper are those of the authors and not necessarily those of the U.S. Naval Ship Systems Command which sponsored the investigation.

Table 1—Chemical Composition of Base Metals[a]

Element	Base metal and heat number: HY-80 19595-1	HY-80 20995	HY-80 69S344	HY-80 N31543	HY-100 73A661	HY-100 N15423	HY-130 3P0074	HY-130 5P0540	HY-130 5P2004	HY-130 5P2456
	Chemical composition, %									
C	0.18	0.15	0.16	0.17	0.15	0.20	0.11	0.12	0.11	0.10
S	0.021	0.019	0.019	0.009	0.016	0.014	0.006	0.003	0.006	0.004
P	0.010	0.018	0.021	0.010	0.012	0.010	0.008	0.004	0.003	0.007
Mn	0.32	0.28	0.33	0.28	0.31	0.30	0.78	0.79	0.88	0.84
Si	0.20	0.25	0.26	0.27	0.22	0.21	0.29	0.35	0.35	0.24
Ni	3.01	2.95	2.86	2.29	2.49	3.00	5.03	4.96	4.95	4.92
Cr	1.47	1.40	1.61	1.31	1.53	1.60	0.56	0.57	0.53	0.54
Mo	0.48	0.41	0.48	0.32	0.36	0.50	0.42	0.41	0.50	0.50
V	—	—	—	—	0.01	—	0.05	0.057	0.08	0.08
Cu	—	0.16	—	0.06	0.04	0.11	—	—	0.07	0.06
Ti	—	—	—	—	0.001	—	—	—	—	0.04
Aℓ	—	—	—	—	—	—	0.015	0.048	—	—

[a] Mill report.

specific measures were taken (stripping of electrode coating, wetting of bare wire, weaving back over a deposit to entrap slag, etc.) to deposit specific types and quantities of flaws in the weldments. Detailed descriptions of the precise techniques used in the deposition of the weld defects are presented elsewhere;[2, 3] however, it should be noted that it was not always possible to hold the defect sizes within the tolerances desired. Thus, several test specimens contained flaw sizes exceeding the nondestructive test (NDT) standards used in the rating of the weldments, as discussed subsequently.

The majority of the butt weldments containing intentionally introduced defects were tested with the weld reinforcement removed. This was accomplished by machining the surfaces of the welded plate in the region of the weld and for several inches to either side thereof, followed by a final polish with a belt sander in the direction of subsequent load application. Removing the weld reinforcement precluded the possibility of fatigue crack initiation at the stress raiser associated with the toe of the weld, thereby permitting evaluation of the effect of the internal defects on the fatigue behavior of the weldments. In addition, the polished surfaces of the test plates permitted higher definition of the internal defects detected by radiography and, where ultrasonic inspection was used, provided a good contact surface between the test plate and the transducer.

The plain plate fatigue specimens of each of the three steels were tested in the as-rolled condition, i.e., with the mill-scale surfaces intact. Although no particular effort was made to protect the plates before testing, the region of the specimen in the vicinity of the test section were inspected visually to insure that no obvious surface nicks were present. The HY-130 plates used later in the investigation were received descaled (grit-blasted) and painted; several plain plate fatigue specimens were tested using this plate stock for comparison with the behavior of the as-rolled material. In addition, the surfaces of several HY-130 specimens were polished before testing as described above for the weldments; this was done to obtain some measure of the difference in fatigue resistance which might be anticipated between a polished laboratory test specimen, and the same material examined in a state more closely resembling an *in situ* condition.

Table 2—Mechanical Properties of Base Metals[a]

Steel	Heat number	Plate thickness, in.	Properties in longitudinal direction: Yield strength[b] ksi	Tensile strength, ksi	Elongation in 2 in., %	Reduction in area, %	Charpy V-notch[c], ft-lb
HY-80	19595-1	1 1/2	80.5	101.1	29.0	74.8	103
	20995	1 1/2	87.3	105.0	25.0	69.4	138
	69S344	1 1/2	88.5	108.3	22.6	69.2	92
	N31543	3/4	90.0	109.2	25.3	70.4	136
HY-100	73A661	3/4	105.9	121.6	22.5	71.5	93
	N15423	3/4	110.0	127.5	23.0	71.1	83
HY-130	3P0074	1/2	138.0	144.0	20.0	69.8	102[d]
	5P0540	1	138.5	149.0	20.5	67.5	83[d]
	5P2004	1	141.6	152.0	20.0	63.8	90[d]
	5P2456	1	140.4	149.2	20.0	64.4	83[d]

[a] Mill report.
[b] 0.2% offset.
[c] At — 120° F unless otherwise noted.
[d] At 0° F.

Nondestructive Test Procedures, Ratings

After fabrication, the welded members were subjected to radiographic inspection at a sensitivity level of two percent. The comparators of Reference 4 were used as interpretive guides to aid in the identification of the internal defects shown on the radiographs. The weldments were then classified as either "acceptable" or "unacceptable" in accordance with the radiographic inspection standards* given in NAVSHIPS Specification 0900-006-9010.[1]

In addition to radiography, ultrasonic inspections were performed on the majority of the HY-130 weldments included in the study. The procedures used were in accordance with NAVSHIPS requirements.[6] However, since the HY-80 specimens tested early in the program were not

* Essentially, these standards of acceptance are based on a one- or two-dimensional expression of defect concentration (i.e., length of slag deposit or lack of fusion: number of dispersed pores: density, alignment, and total weld area reduction for clustered porosity, etc.). For example, a 6 in. length of weld in a 1 in. thick plate may exhibit a maximum length of lack of fusion or lack of penetration of 0.167 in. for an individual indication, or a total accumulated length for multiple, aligned indications of 0.417 in. For elongated slag deposits, the maximum acceptable length of an individual indication is 0.375 in. and, for multiple aligned indications, the total permissible accumulated length is 1 in. The limitations on dispersed pores are based on a combination of size, density, and total defect area. For a 1 in. thick plate a 6 in. length of weld may contain a maximum of 21 dispersed pores of assorted sizes varying in diameter from 0.0275 in. to 0.125 in., lowering to a maximum of 5 pores if all are approximately of 0.125 in diameter. Regardless of size distribution, the maximum area of porosity may not exceed 1% of the weld cross-sectional area (plate thickness x length of weld). Pores are considered "clustered" when a group of five or more pores can be circumscribed by a circle of 0.5 in. diameter (for a 1 in. plate), such clusters being considered unacceptable if the sum of the diameters of the pores in the group exceeds 0.5 in. Restrictions are also placed on the alignment of individual pores, with such restrictions including a measure of the number, size, and total included length of the pores in the group, as well as the proximity of the group of indications to another aligned group. For both the clustered porosity and the aligned pores, the same 1% limitation on total porosity area noted above is applicable as an additional criterion for acceptance. Finally, all indications of weld cracking are considered unacceptable by the standards.

The HY-130 weldments were rated, with respect to limitations on porosity, in accordance with recommendations proposed by the U. S. Steel Corporation.[5]

inspected ultrasonically, only the radiographic inspection results were used in rating the weldments fabricated from each of the three steels. Additionally, both ultrasonics and radiography were utilized in an attempt to determine the time to initiation of fatigue cracks at internal weld defect sites, and to obtain a measure of the propagation of such cracks before they penetrated the plate surfaces. The results of this study are presented by the authors in a companion paper.[7]

Test Procedure

Details of the plain plate and of the butt-welded fatigue specimens are shown in Fig. 1. The welded specimens were tested with the axis of the weld oriented normal to the direction of loading, thereby subjecting the entire cross-section of the weld to the same range of stress. The width of the specimens in the test section varied from 2 to 4 in., depending upon the thickness of the test plate and the magnitude of the desired stresses; the width was made as large as possible within the capacity of the test equipment.

The fatigue tests were conducted under pulsating tension loading (stress ratio, $R = S_{min}/S_{max} = 0$). All specimens were tested in 200,000 lb capacity Illinois' lever-type fatigue machines which operate at a speed of approximately 150 cpm. A diagram of the essential features of the testing machines is shown in Fig. 2.

Fatigue failure was taken as the number of cycles at which a crack progressing through the test specimen caused a preset micro-switch to shut off the testing machine. Cycling was continued at reduced loads until complete fracture occurred so that the fracture surfaces of the specimen could be exposed and examined. In all cases, less than a 1% increase in fatigue life was obtained from the time of machine shut-down to complete rupture.

Analysis of Data

For materials subjected to constant amplitude, controlled stress cycling, a linear log-log relationship generally may be established empirically between applied stress and fatigue response for failures occurring over several orders of magnitude of life. In the present study, regression analyses of the fatigue data obtained from tests of each of the various specimen types were performed by applying the method of least squares[8] to the linear logarithmic expression between fatigue life, N, and applied (nominal) stress, S:

$$\log N = C + m \log S \quad \text{or} \quad N = k S^m \qquad [1]$$

where $k = \log^{-1} C$. Both k and m are considered empirical constants which are dependent upon the materi-

Table 3—Chemical Composition of Electrodes Used for Welding HY-130 Steel

Electrode designation	AX-140[a]	5Ni-Cr-Mo[b]	L140[c]	M14018[d]	
Heat number	1P0047	50646	106140	1P1375	
Electrode type	Bare wire	Bare wire	Bare wire	Covered electrode	
Electrode diameter, in.	1/16	1/16	1/16	5/32	3/16
Element	Chemical composition, %				
C	0.097	0.11	0.11	0.077	0.081
S	0.007	0.006	0.007	0.003	0.004
P	0.006	0.004	0.008	0.003	0.003
Mn	1.85	0.75	1.72	1.91	1.85
Si	0.30	0.38	0.36	0.42	0.39
Ni	2.10	5.03	2.49	2.08	1.92
Cr	0.91	0.61	0.72	0.71	0.73
Mo	0.54	0.47	0.88	0.43	0.43
V	—	0.01	0.01	—	—
Cu	—	—	0.08	—	—
Ti	0.01	0.015	—	—	—
Al	0.018	0.01	—	—	—
N	0.013	0.004	—	—	—
O	0.015	—	—	—	—

[a] Air Reduction Co.,
[b] U. S. Steel Corp.
[c] Linde Division, Union Carbide Corp.
[d] The McKay Company.

Table 4—Procedures for Preparation of Butt Welds

Welding parameters	Base metal						
	HY-80	HY-100		HY-130			
Electrode	E11018	E11018	E12018	AX-140[a]	5Ni-Cr-Mo[b]	L140[c]	M14018[d]
Welding process[e]	SMA	SMA	SMA	GMA	GMA	GMA	SMA
Electrode diameter, in.	5/32, 3/16	5/32, 3/16	5/32, 3/16	1/16	1/16	1/16	5/32, 3/16
Current, amp	130–220	130–220	130–220	290–340	290–320	285–330	150–210
Voltage, v	21	21	21	29	28, 29	28, 29	22
Preheat temperature, °F	150	150	150	275	200	225	200
Interpass temperature, °F	200	200	200	225	200	225	200
Max. heat input, kjoules/in.	40	40	40	45	45	45	37.5
Arc travel speed, ipm	5–8	5–8	5–8	13, 16	13, 14	13, 14	6–8
Shielding gas	—	—	—	Argon, 2% O_2	Argon, 2% O_2	Argon, 2% O_2	—
Joint geometry	Double vee 60 deg. incl. angle	Double vee 60 deg. incl. angle	Double vee 60 deg. incl. angle	Double vee 60 deg. incl. angle	Double vee 60 deg. incl. angle	Double vee 60 deg. incl. angle	Double vee 60 deg. incl. angle

[a] Air Reduction Co.
[b] U. S. Steel Corp.
[c] Linde Division, Union Carbide Corp.
[d] The McKay Company.
[e] SMA—shielded metal-arc; GMA—gas metal-arc.

Table 5—Fatigue of HY-130 Plain Plates—0 to 80 ksi Stress Cycle

Mill-scale intact		Polished		Descaled and painted	
Specimen no.	Life, cycles	Specimen no.	Life cycles	Specimen no.	Life, cycles
NA-1	64,200	NA-13	304,300	NE-1	330,800
NA-2	60,900	NA-15	208,800	NE-5	252,700
NC-13	59,800			ND-3	249,000
NA-5	51,100			ND-2	187,800
NC-14	50,500				
Avg.	57,300	Avg.	256,500	Avg.	255,100

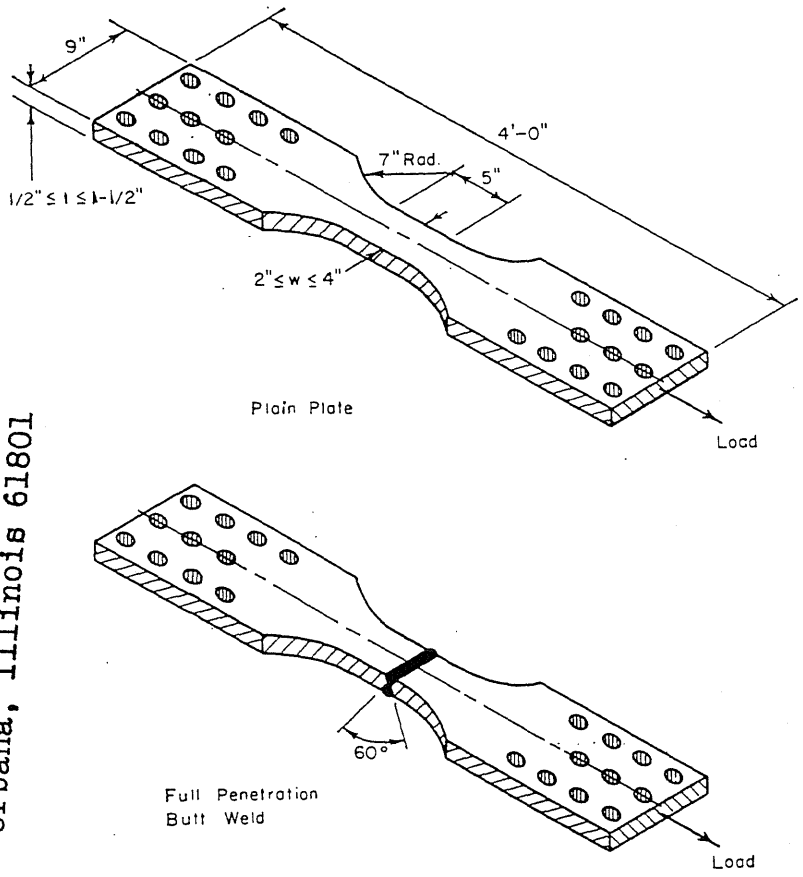

Fig. 1—Details of the fatigue test specimens

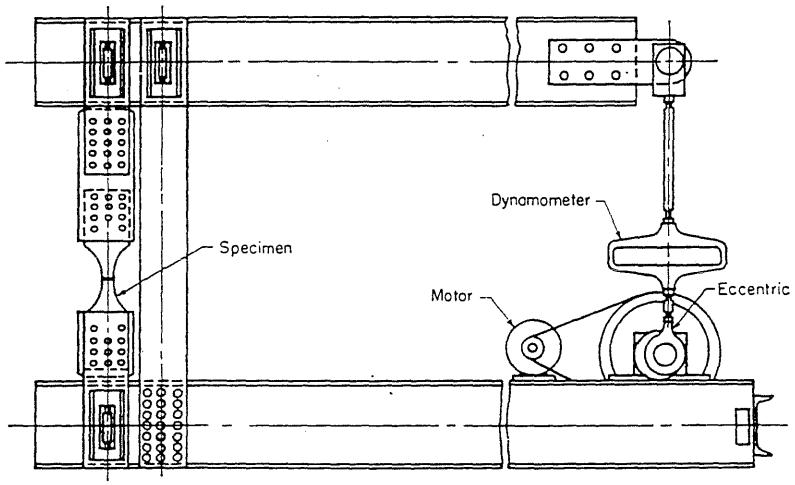

Fig. 2—Schematic diagram of fatigue testing machine

al and the type of specimen being tested, as well as upon the nature of the loading spectrum.

S-N curves were generated with the above relationship using data for specimens tested at cyclic stresses equal to or below the nominal material yield strength as the upper limit, and for stresses resulting in fatigue lives on the order of 2 x 10^6 cycles at the lower limit.

Test Results and Discussion

Plain Plates

The fatigue results for plain plate specimens tested with mill-scale intact are shown in Fig. 3 for the three grades of steel examined. As seen in Fig. 3, the fatigue lives at the several stress levels are quite similar for the three steels. Since analysis of the data sets for each of the steels individually resulted in essentially coincident regression lines, a single S-N curve was generated to represent the combined data for all of the as-rolled plates. This similarity of response among the three steels was found to extend to the butt weldments as well; subsequent discussions of the cyclic behavior of the welded joints thus may be considered equally applicable to each of the materials.

It should be noted that the single curve of Fig. 3 is representative of the combined data specifically for the surface condition (mill-scale intact) considered. Schwab and Gross,[9] and Haak, *et al.*[10] found that, for polished rotating beam specimens tested in air, fatigue strength increased with increasing tensile strength for lives beyond approximately 10^4 cycles to failure. This suggests, then, that surface condition influences considerably the fatigue response of these materials, especially with regard to the number of cycles undergone prior to crack initiation.

Effect of Surface Finish. To obtain a measure of the effect of surface finish on fatigue, HY-130 specimens were tested with plate surfaces either polished or descaled (grit-blasted) and painted. These tests, conducted at a stress cycle of 0 to +80 ksi, resulted in an average fatigue life of 255,000 cycles for both treatments, or a fourfold increase in life over the average exhibited by the specimens tested with the mill-scale intact, as seen in Table 5. Similar variations in fatigue resistance between as-rolled and polished plates have been reported for other high-yield-strength steels as well.[11]

Examination of the fracture surfaces after testing generally revealed single crack initiation sites for the polished and for the descaled and painted specimens, usually occurring at or near a corner of the test section. The as-rolled HY-130 plates, however, contained a loose mill-scale surface underlain by a coarse oxidized layer (see Fig. 4), the surface of which served as the site for the formation of multiple fatigue cracks dispersed over the entire specimen test section. Following the coalescence of several such cracks into a single, continuous line, propagation then progressed through the cross-section of the specimen. Since the rate of crack propagation has been found to be very nearly the same for the HY-80 and HY-130 steels,[12, 13] the similarity in fatigue response of the as-rolled plates of the three materials may be attributable to a like number of cycles being required to initiate cracking (on a macroscale), such initiation, in turn, being governed by the plate surface conditions. Also, with the HY-130 specimens, the plate surface treatments were apparently responsible for delaying the initiation of fatigue cracking, thereby providing the increased fatigue lives reported in Table 5.

From the above, it is evident that the fatigue behavior of these high-strength steels, to be fully described, must be expressed not only in terms of the applied stresses, but by the type and condition of the test specimen (and testing environment) as well.

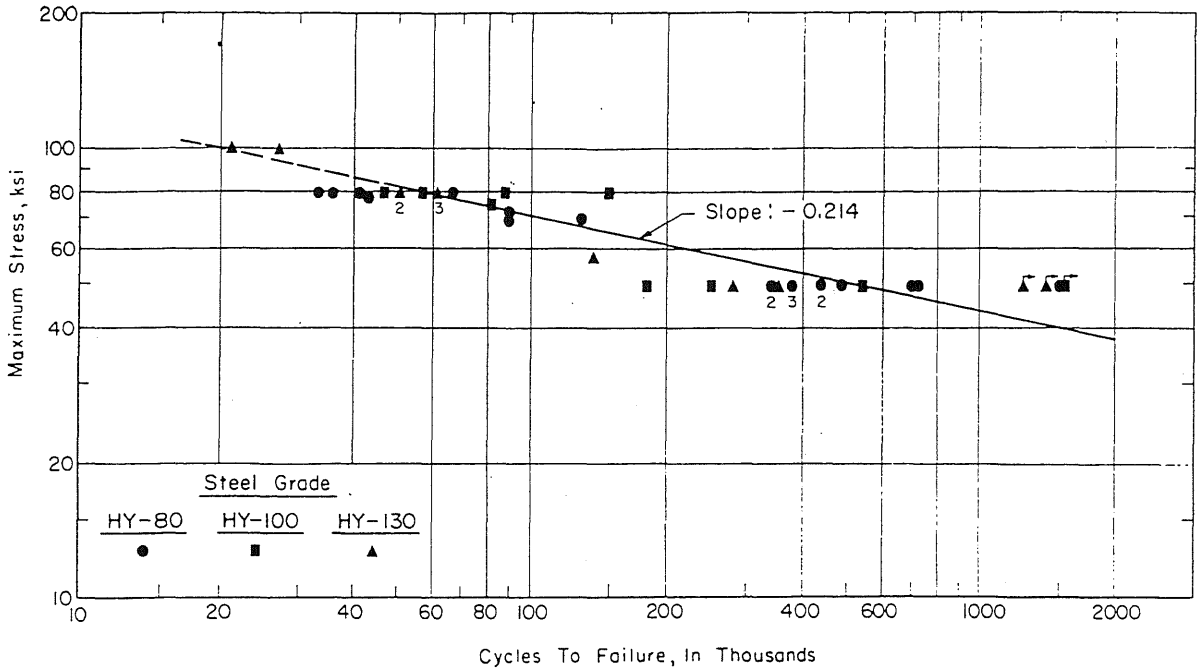

Fig. 3—Fatigue test data and S-N curve for plain plate specimens with mill-scale intact. Numbers adjacent to the data points indicate the failure of two or more specimens of one steel at approximately the same lives

Butt Welds

A summary of the fatigue tests of the butt-welded specimens (both as-welded and with the weld reinforcement removed) fabricated using each of the three base metals is presented in Table 6. The nondestructive test ratings are based on the results of radiographic inspection; specimens failing the radiographic standards were tested without repair to provide some indication of the applicability of the standards in designing for fatigue.

Toe Initiated Failures. The fatigue test results for the butt-welded specimens initiating failure at the toe of the weld are shown in Fig. 5. As with the plain plates, the data for the three steels have been combined to generate a single S-N curve. A photograph of a typical fracture surface for a specimen in which failure initiated at the weld toe is shown in Fig. 6.

The range of fatigue lives obtained at each of the stress levels used is within the normal scatter expected of specimens having a common joint geometry and similar weld reinforcement contour. Comparison of the behavior of the weldments exhibiting toe initiated failures with the S-N curve data for the plain plates in Table 7 shows a marked reduction in fatigue strength for the as-welded specimens at the longer lives corresponding to nominal stresses which are well within the elastic range of each of the three steels. At 500,000 cycles, for example, a fatigue strength of 27.5 ksi is indicated by the S-N curve for the as-welded specimens, or just slightly more than half the 50 ksi fatigue strength found for the base metal. This significant difference in behavior between the as-welded and the plain plate specimens is attributable in part to the earlier activation of fatigue cracking in the weldments, resulting from the concentration of stress introduced by the geometry at the toe of the weld.

The difference between the fatigue resistance of the butt-weldments exhibiting failure at the toe of the weld and the base metal specimens diminishes at shorter lives corresponding to the higher stress amplitudes. In this low cycle region, the number of cycles to crack initiation was observed to occupy a proportionately smaller percent of the total life of a specimen than at the lower stress levels. With the major portion of life thus spent in crack propagation at the high stress

Fig. 4—Photomicrograph of HY-130 plain plate with mill-scale surface intact. X750 (reduced 44% on reproduction)

Table 6—Summary of Fatigue Test Results —Butt Welded Specimens

Steel	Condition	Radiographic survey — Rating	No. tests	Site of fatigue crack initiation, no. tests — Toe of weld	Dispersed pores, porosity	Slag, elong. voids	Lack of fusion or penetration	Multiple defects	Other[a]
HY-80	As-Welded	Pass	11	11	0	0	0	0	0
		Fail	4	4[b]	0	0	0	0	0
	Reinforcement Removed	Pass	33	—	16	9	0	0	8
		Fail	28	—	7	11	5	4	1
HY-100	As-Welded	Pass	26	16	7	0	3	0	0
		Fail	0	0	0	0	0	0	0
	Reinforcement Removed	Pass	12	—	7	0	0	0	5
		Fail	4	—	3	0	0	1	0
HY-130	As-Welded	Pass	35	12	2	0	13	2	6
		Fail	6	2	1	0	0	2	1
	Reinforcement Removed	Pass	26	—	4	3	7	4	8
		Fail	19	—	4	5	5	3	2

[a] On base metal surface removed from region of weld; at cracks perpendicular to weld axis; in nugget papilla of weld bead; etc.
[b] Cracking initiated at weld undercut.

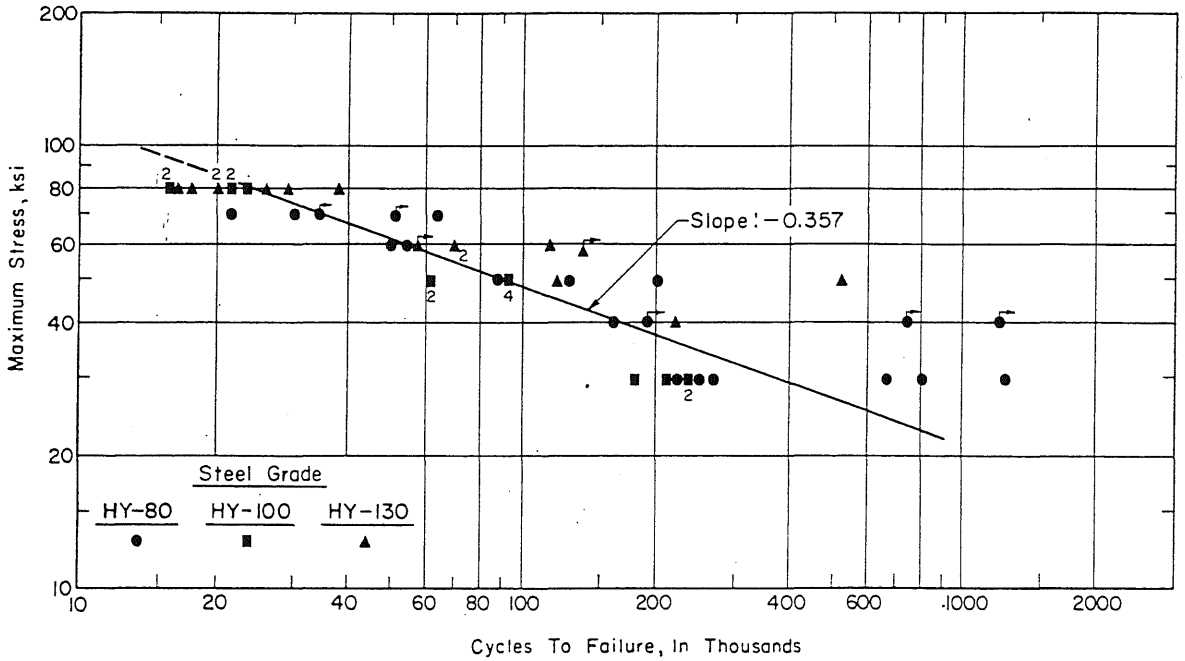

Fig. 5—Fatigue test data and S-N curve for butt welds (as-welded) exhibiting crack initiation at the toe of the weld. Data points marked with an arrow represent as-welded specimens in which failure initiated at some other location (e.g., at an internal defect, or in test specimen pull-head) but which had lives at least equivalent to those of specimens exhibiting toe failures

amplitudes, the similarity in behavior of the plain plates and the weldments is to be expected. Moreover, if only the crack propagation phase of the total fatigue lives is considered, the two specimen types should exhibit essentially the same behavior.

Internally Initiated Failures. The fatigue test results for all butt-welded specimens in which fatigue cracking initiated internally are shown in Fig. 7. The data are for specimens both as-welded and with the weld reinforcement removed, and which were rated acceptable in accordance with the radiographic standards used. Also shown are the S-N curves for the plain plate specimens, and for the butt-weldments which exhibited failure at the toe of the weld. Photographs of typical specimens initiating fatigue cracking at the site of various internal defects are shown in Fig. 8.

The most significant aspect of the data presented in Fig. 7 is the very large scatter in fatigue lives at the several stress levels investigated, exceeding two orders of magnitude of life at a stress cycle of 0 to +50 ksi. Such wide variations in life are not unexpected in view of the many different types (and sizes) of internal weld discontinuities present at the crack initiation sites—Table 6. To ascertain if a particular type of defect was associated primarily with failures occurring at either extreme of the range of lives observed for tests conducted at one stress level, the fatigue data have been grouped by defect type and compared, in Figs. 9 and 10, for maximum cyclic stresses of 50 ksi and 80 ksi, respectively.

The defect types specified in Figs. 9 and 10 are those actually observed at the internal crack initiation sites regardless of the radiographic descriptions of the weldments. These defects were not always the ones which appeared to be most severe on inspection prior to cycling. Consequently, when the fatigue data for specimens failing the nondestructive test standards are included in the comparisons of Figs. 9 and 10, they are seen often to have exhibited lives equal to or exceeding the lives of specimens rated as acceptable by the standards. The role of nondestructive testing in the estimation of fatigue response is discussed in detail later.

Inspection of Figs. 9 and 10 shows that the scatter in fatigue lives of specimens initiating internal cracking is only slightly diminished when the individual defect types are considered. Nor can the wide ranges of lives be attributed to differences among the three steels, as indicated by Fig. 11, wherein the data for failures initiating at both spheroidal and planar-type defects are presented for each steel individually. It was found also that there were no differences in fatigue behavior which could be related to one or another of the several electrodes used in the preparation of the HY-130 weldments, when failure initi-

Fig. 6—Photograph of fracture surface of butt-welded specimen in which fatigue cracking initiated at the toe of the weld

Table 7—Comparison of Fatigue Strengths of Plain Plates and Butt Welds

Type of specimen	Fatigue life, cycles	Fatigue strength, ksi	Percent of plain plate fatigue strength
Plain plate, mill-scale intact	20,000	100	—
	100,000	71	—
	500,000	50	—
	2,000,000	37.5	—
Butt weld, as-welded (failure at toe of weld)	20,000	86	86
	100,000	48.5	68
	500,000	27.5	55
	2,000,000	(16.5)[a]	44

[a] Estimated.

ated at like defects. About the only conclusion afforded by the comparisons in Figs. 9 through 11 is the broad generalization that the planar discontinuities can be somewhat more deleterious to the fatigue strength of a welded joint than the spheroidal defect configurations associated with porosity.

It would be reasonable to assume that the total fatigue life of a weld containing internal discontinuities is dictated by a variety of interacting factors, including the dimensions of the defects, the proximity of one defect to another and to the surface of the test specimen, and, for certain states of applied stress, the nature of the residual stress field. For the weldments tested in this program, an attempt was made to correlate, for an individual type of defect, defect size with fatigue life at a specific stress level. In Fig. 12, the fatigue lives of specimens initiating fatigue cracking at clustered porosity are compared on the basis of a simple two-dimensional representation of the cluster (i.e., the total area of all pores in the cluster observed on the weld fracture surface, reported as a percentage of the specimen cross-sectional area).

Although a certain trend toward a reduction in fatigue life with increasing defect area may be seen, the trend is far from convincing. An even less consistent correlation was encountered when the specimens were compared on the basis of defect area measured from radiographs obtained by X-raying at normal incidence to the surface of the specimen. This was to be expected, for cracks initiating at one elevation in the weldment (on a plane through the weld and perpendicular to the faces of the specimen) would progress normal to the direction of loading and be relatively unaffected by the presence of pores located at other elevations. It is evident, therefore, that a planar measure of defect density such as total area reduction, although adequately quantifying the degree of deviation of a weld from complete soundness and, presumably, offering a measure of the integrity of the weld under static load, cannot in itself be used to reliably predict the total performance of the weldment under cyclic loading.*

A similar comparison between defect size and fatigue life, for welds containing lack of fusion or lack of penetration, is presented in Fig. 13, where the ordinate is the length of the discontinuity parallel to the weld axis, measured on the specimen fracture surface. As with the clustered porosity, it can be seen from Fig. 13 that this measurement was not a particularly reliable indicator of fatigue behavior, at least for specimens on the order of an inch or less in thickness and for which failure is assumed to have occurred when a crack has progressed through the thickness of the plate.

Stages of Initiation and Propagation of Cracks Originating at Internal Defects. If neither defect length nor area as defined above are satisfactory indicators of cyclic response for weldments exhibiting internal crack initiation, the question remains as to whether some one- or two-dimensional parametric quantities representative of an internal defect can be satisfactorily used to estimate fatigue behavior. The results of a companion study[7] have indicated that the duration of crack *propagation* could be reasonably well described in terms of the through-thickness dimension of the defect at the initiation site, the proximity of the defect to the surface of the specimen, and the ratio of defect (initial crack) width to specimen thickness. With the notch geometry at the tip of an advancing fatigue crack being the same regardless of the configuration of the original defect at the initiation site, it was possible to apply fracture mechanics concepts to relate the rate of crack propagation to crack width and nominal applied stress, the total number of cycles of propagation available before failure then becoming a function of plate thickness and the distance from the crack to the specimen surface. For specimens containing identical defect types (having similar boundary geometries which could be expected to foster crack initiation at the same number of cycles at a given nominal

* This observation is limited to the conditions considered in this study, i.e., the behavior of weldments in which the area reductions for porosity are of the order of 1% or less. Other investigators have reported a reasonable correlation between fatigue life and defect area for area reductions between approximately 1 and 15%.[14]

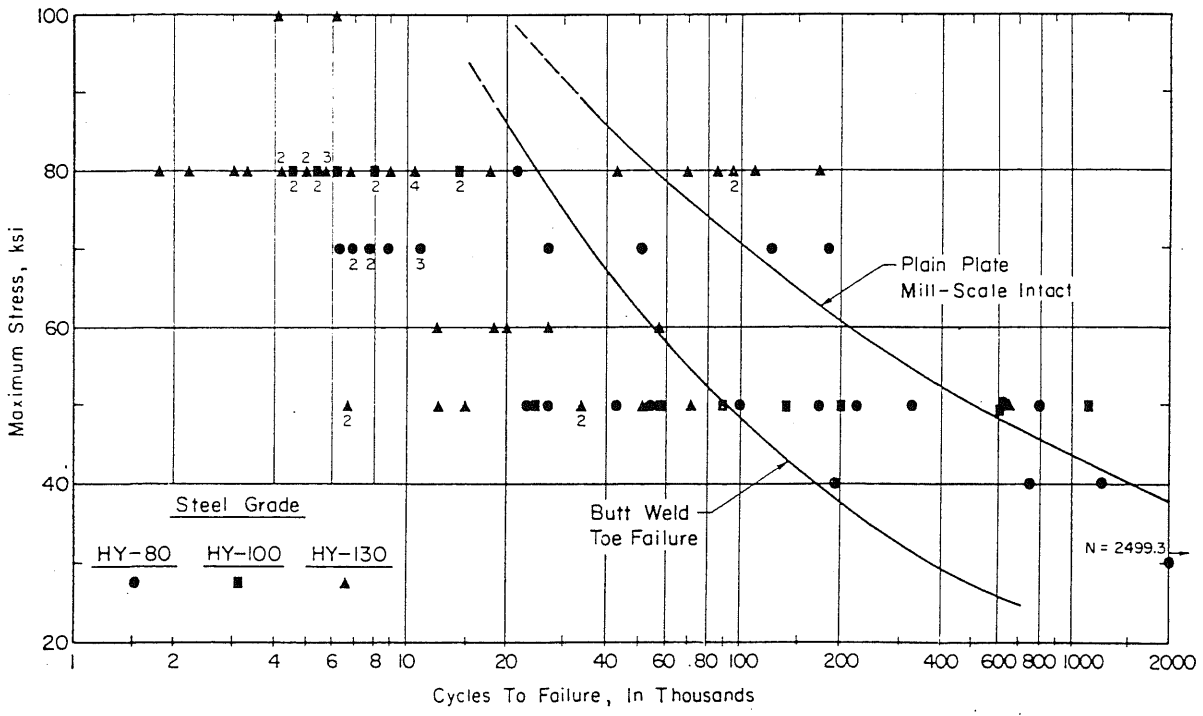

Fig. 7—Fatigue test data for butt-welded specimens exhibiting crack initiation at internal weld discontinuities. S-N curves for plain plates, and for butt welds exhibiting toe failures are also presented. (Semi-logarithmic coordinate axes used)

stress), the total fatigue lives would be expected to vary as an inverse function of the through-thickness dimension of the initial defect. This in fact was the case, as seen in Fig. 13, where four specimens containing continuous lines of incomplete penetration and tested at a stress cycle of 0 to +50 ksi exhibited fatigue lives varying from approximately 10^4 to 10^5 cycles, the shorter lives associated with the wider defect bands and vice versa.

Although the crack propagation stage of the fatigue life of specimens exhibiting internal crack initiation can be reasonably well defined as indicated above, the number of cycles required to initiate active (macroscopic) cracking at a defect site is more difficult to ascertain.[7] This arises in part from the difficulty encountered in quantifying those parameters critical to crack nucleation, especially the notch geometry at the defect boundary which will, in turn, dictate the local cyclic strain history in the material immediately adjacent to the flaw. For example, in some of the specimens tested, crack initiation was encountered at a single pore well removed from a seemingly more critical cluster of porosity; in other specimens cracking initiated along a short line of incomplete fusion encompassed by a porosity cluster and hidden from nondestructive test detection by the cluster.

It is difficult to establish a reasonable measure of the number of cycles necessary to initiate an active (macroscopic) fatigue crack at a specified stress level. For this reason it may be well to consider only the propagation stage in estimating the response of a weldment under repeated loads. At stresses approaching the yield strength of the test material, such an approach may be reasonable. This is because the attendent high rates of propagation would render the consequences of failing to detect a small but severe discontinuity quite critical, since early initiation could result in extensive crack growth before a routine periodic service inspection were performed.

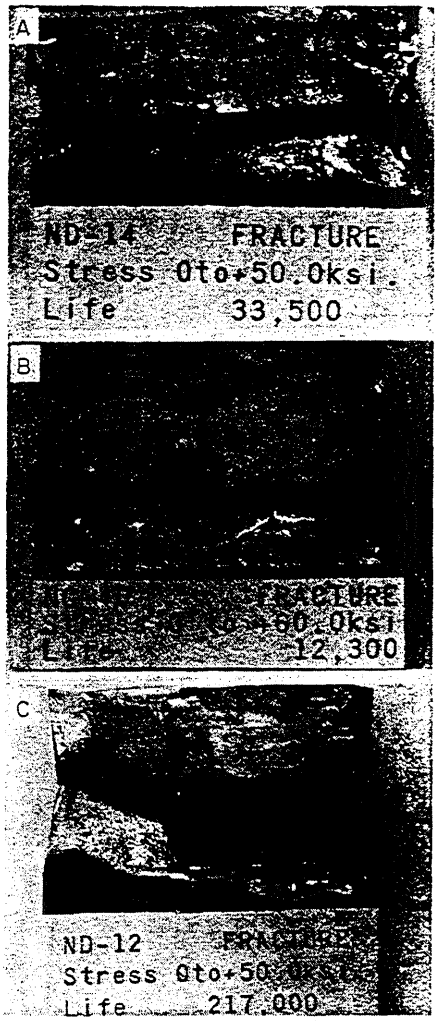

Fig. 8—Photographs of fracture surfaces of butt-welded specimens in which fatigue cracking initiated at: A—porosity; B—slag inclusions; C—lack of fusion

At lower nominal stresses, the use of only the crack propagation life may seem unduly conservative, for the number of cycles of load application before initiation could occupy a proportionately larger part of the specimen's total fatigue life. However, at the lower stresses, toe failures may become relatively more critical—Fig. 7. In such cases, design stresses based on a regression curve for members failing at the toe of the weld, using an appropriate factor of safety, may be adequate to cover the range of lives encountered with internally initiated failures as well.

Application of NDT Standards to Estimation of Fatigue Behavior

Acceptance standards based on the data obtained from such nondestructive test (NDT) techniques as radiography and ultrasonics traditionally have been used as a means of limiting the types and concentration of internal discontinuities permitted in a weld, thereby ensuring the integrity of the welded member or structural component under a single application of load. The effectiveness of these standards as measures of the resistance of the weldments to repeated loads, however, bears further examination.

When the presence of appreciable concentrations of such defects as clustered porosity, slag inclusions, or continuous lines of incomplete fusion was clearly distinguished by radiography, fatigue crack initiation generally occurred at these defects in the weldments subjected to axial fatigue. Exceptions to this rule were not uncommon, however, especially for weldments in the higher strength HY-130 steel; for example, it was found that cracking occasionally initiated at a single, isolated pore or at a small planar defect even when the presence of other larger flaws was indicated on the radiographs. Further, several specimens classified as "sound" (defect-free) weldments by radiographic inspection failed at internal locations containing intermittent lack of fusion, very small pores or, for the HY-130 gas metal-arc welds, in the region of deep weld bead penetration (nugget papilla) common to weldments fabricated using the gas metal-arc process

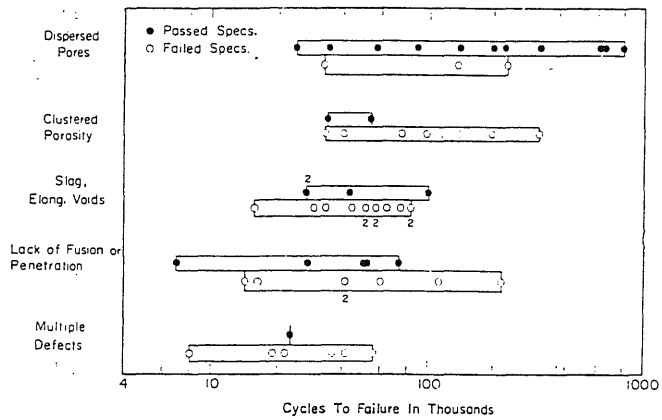

Fig. 9—Influence of various defect types on the fatigue behavior of butt-welded specimens at a stress cycle of 0 to +50 ksi

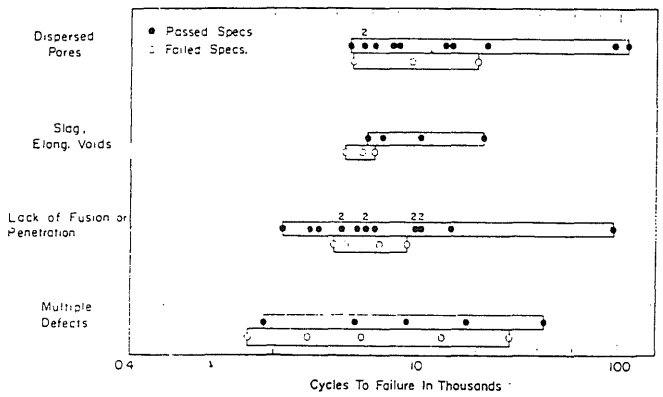

Fig. 10—Influence of various defect types on the fatigue behavior of butt-welded specimens at a stress cycle of 0 to +80 ksi

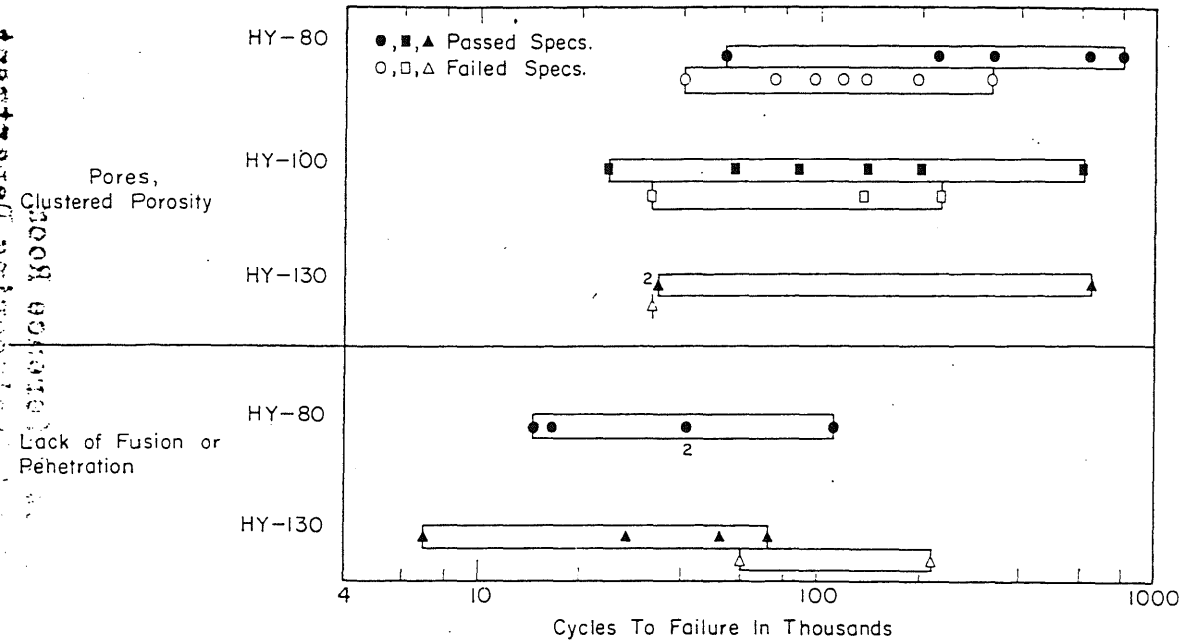

Fig. 11—Influence of grade of steel on the fatigue behavior of butt-welded specimens exhibiting crack initiation at internal defects. Tests conducted at a stress cycle of 0 to +50 ksi

and the argon-oxygen shielding gas.[15]

Even if it were possible to select, from the results of a nondestructive testing inspection, the site at which fatigue cracking would be most likely to initiate, it was found that the *type* of defect at the crack origin could not be used reliably as the basis for estimating the expected fatigue life of the weldment. It was found, further, that the dimensional parameters of defect severity commonly used for standards of acceptance by radiography (e.g., size and density of porosity as expressed by total defect area, or length of incomplete fusion or penetration in the direction of the weld axis) offered only a slightly better correlation with total fatigue life. Such quantities, by themselves, appear to be inadequate as a foundation upon which to establish standards relevant to the design, for repeated axial loads, of the type of weldments examined herein.

For welded members and details in which fatigue failure is defined as the number of cycles at which a crack has penetrated through the thickness of the plate, it was noted earlier that the *propagation* phase of the total lifetime could be estimated with some reliability if the through-thickness dimension of the crack-initiating defect, the proximity of the defect to the plate surface, and the cyclic stress can be determined. It would seem reasonable, then, to use the above parameters for establishing quality standards required of weldments designed to withstand a finite number of load cycles; such standards would be conservative, for only the propagation life fraction would be used. Because of the difficulty in estimating the number of cycles to crack initiation, it would normally be unwise to depend upon that segment of the total fatigue life in design.

Conclusion

The behavior under repeated axial

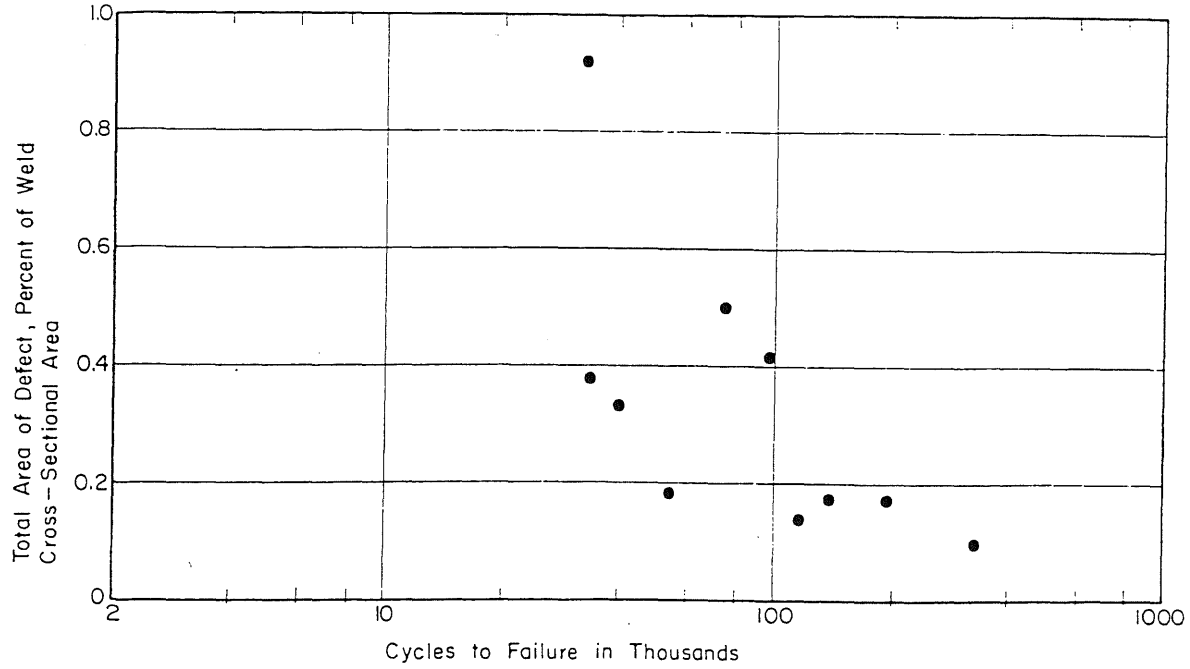

Fig. 12—Variation in fatigue life with defect area for specimens initiating failure at clustered porosity. Tests conducted at a stress cycle of 0 to +50 ksi

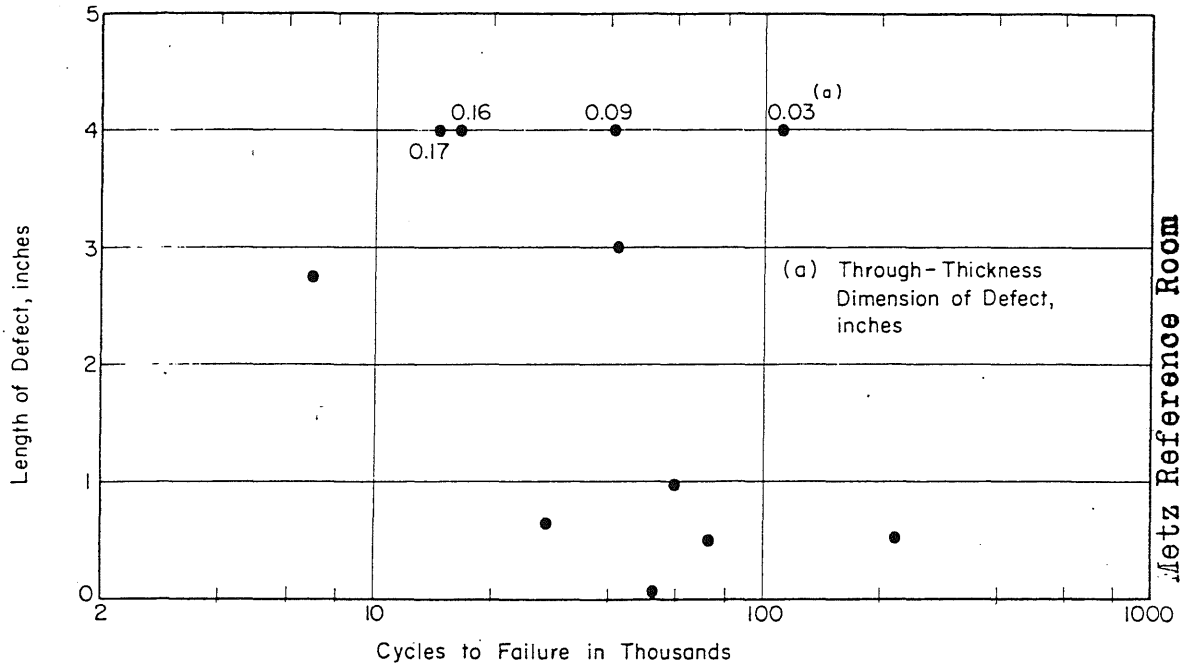

Fig. 13—Variation in fatigue life with defect length for specimens initiating failure at lack of fusion or lack of penetration. Tests conducted at a stress cycle of 0 to +50 ksi

loads of plain plates and butt weldments of three high-yield-strength steels—HY-80, HY-100 and HY-130—has been studied. The results of the fatigue tests, using a stress cycle of zero-to-tension, have indicated the following:

Within the range of lives from approximately 10^4 to 10^6 cycles, the fatigue behavior of the plain plate specimens (with mill-scale surface intact) was similar for the three steels, and could be described by a single S-N curve. Surface condition was found to have a marked effect on the fatigue resistance of the base metal specimens. For the HY-130 material, the fatigue lives of polished plates and those with descaled and painted surfaces were essentially the same; at a stress cycle of 0 to +80 ksi, the average life of the plates with treated surfaces was four times the average for plates with mill-scale intact.

The fatigue behavior of butt weldments (as-welded) of HY-80, HY-100 and HY-130 steel in which crack initiation occurred at the toe of the weld reinforcement could be represented by a single S-N curve. For these weldments, the reduction in fatigue strength relative to the behavior of the plain plate specimens was most pronounced at the longer lives reflecting, in part, the earlier initiation of fatigue cracking in the welds at the stress raiser provided by the toe of the reinforcement. At 500,000 cycles, the average fatigue strength of the welded specimens was 27.5 ksi, in comparison to the 50 ksi fatigue strength of the plain plates.

Wide variations in fatigue life at all test stress levels were exhibited by butt-welded specimens in which cracking initiated at internal weld discontinuities. The scatter in lives could not be explained solely on the basis of the type of weld defect initiating failure, nor could it be attributed to differences in the base metal, the weld metal or the welding process. Further, the one- or two-dimensional characteristics of the defect which are commonly used as the basis for radiographic nondestructive testing acceptance standards were found to be largely inappropriate for estimating the total life expectancy of a weldment with internal flaws. The test data have indicated, however, that the fraction of the total life spent in (macroscopic) crack propagation could be estimated with reasonable reliability if the through-thickness dimension (width) of the crack-initiating defect, the position of the defect relative to the specimen surface, and the nominal cyclic stress were known.

Acknowledgments

The tests reported in this study are the result of an investigation conducted in the Civil Engineering Department of the University of Illinois at Urbana-Champaign, Illinois. The program was sponsored by funds provided by the Naval Ship Systems Command, U.S. Navy.

This investigation constitutes a part of the structural research program of the Department of Civil Engineering, of which Dr. N. M. Newmark is the Head. The program was conducted under the general supervision of W. H. Munse, Professor of Civil Engineering.

The authors wish to thank the many staff members at the University who have assisted in the conduct of this investigation.

References

1. NAVSHIPS Specification No. 0900-006-9010, "Fabrication, Welding and Inspection of HY-80 Submarine Hulls," Naval Ship Engineering Center, Navy Department, Washington, D.C., June 1966.

2. Zimmerman, J. E., Jr., and Munse, W. H., "Fatigue Behavior of Defective Welded Joints in HY-80 Steel Subjected to Axial Loadings," Civil Engineering Studies, Structural Research Series No. 252, University of Illinois, Urbana, Illinois, July 1962.

3. Hartmann, A. J., Bruckner, W. H., Mooney, J., and Munse, W. H., "Effect of Weld Flaws on the Fatigue Behavior of Butt-Welded Joints in HY-80 Steel," Civil Engineering Studies, Structural Research Series No. 275, University of Illinois, Urbana, Illinois, December 1963.

4. "Guide for Interpretation of Non-Destructive Tests of Welds in Ship Hull Structures", Ship Structure Committee Report SSC-177, Prepared by National Academy of Sciences—National Research Council, Washington, D. C., September 1966.

5. Porter, L. F., Rathbone, A. M., *et al.*, "The Development of an HY-130(T) Steel Weldment", Applied Research Laboratory Report No. 39.018-001(64), U. S. Steel Corporation, Monroeville, Pa., July 1966.

6. NAVSHIPS Specification No. 0900-006-3010, "Ultrasonic Inspection Procedure and Acceptance Standards for Production and Repair Welds", Naval Ship Engineering Center, Navy Department, Washington, D. C., January 1966.

7. Lawrence, F. V., Jr. and Radziminski, J. B., "Fatigue Crack Initiation and Propagation in High-Yield-Strength Steel Weld Metal", Paper contributed for presentation at the AWS 51st Annual Meeting, Cleveland, Ohio, June 8-12, 1970.

8. Reemsnyder, Harold S., "Procurement and Analysis of Structural Fatigue Data", *Journal of the Structural Division*, ASCE, Vol. 95, No. ST7, Proc. Paper 6693, July 1969, pp. 1533-1551.

9. Schwab, R. C., and Gross, M. R., "Fatigue Properties of 5 Ni-Cr-Mo-V, HY-130/150 Steel", MEL R&D Phase Report

365/65, U. S. Navy Marine Engineering Laboratory, Annapolis, Md., October 1965.

10. Haak, R. P., Loginow, A. W., and Rolfe, S. T., "Rotating-Beam Fatigue Studies of Experimental HY-130/150 and HY-180/210 Steels", Applied Research Laboratory Report No. 40.018-001(32), U. S. Steel Corporation, Monroeville, Pa., December 1964.

11. Haaijer, Geerhard, "Design Data for High-Yield-Strength Alloy Steel", *Journal of the Structural Division*, ASCE, Vol. 92, No. ST4, Proc. Paper 4887, August 1966, pp. 31-49.

12. Crooker, T. W., and Lange, E. A., "Low Cycle Fatigue Crack Propagation Resistance of Materials for Large Welded Structures", *Fatigue Crack Propagation*, ASTM STP 415, Am. Soc. Testing Matls. 1967, pp. 94-126.

13. Barsom, J. M., Imhof, E. J., Jr., and Rolfe, S. T., "Fatigue-Crack Propagation in High-Strength Steels", Applied Research Laboratory Report No. 39.018-007(27), U.S. Steel Corporation, Monroeville, Pa., December 1968.

14. Burdekin, F. M., Harrison, J. D., and Young, J. G., "The Effect of Weld Defects with Special Reference to BWRA Research", *Welding Research Abroad*, Welding Research Council, Vol. XIV, No. 7. August-September 1968. Reprinted from the *Australian Welding Journal*, January 1968.

15. Enis, A., and Telford, R. T., "Gas Metal-Arc Welding of HY-130(T) Steel," WELDING JOURNAL, 47(6), Research Suppl., 271-s to 278-s (1968).